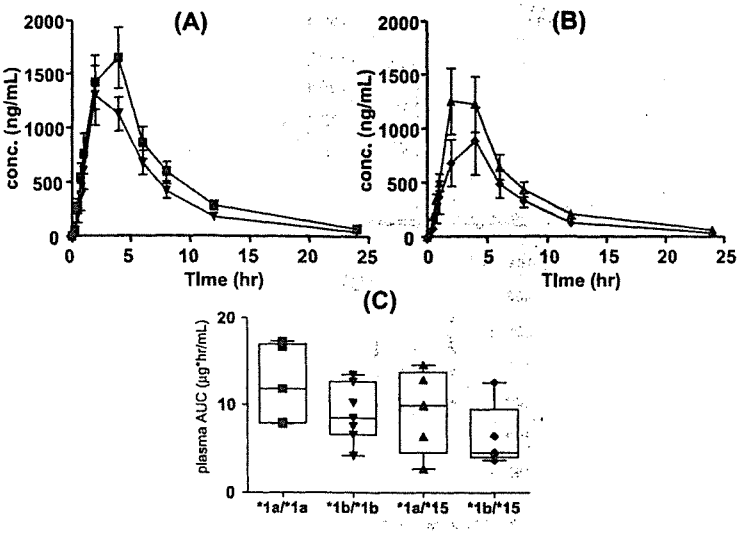

Fig 2. Effect of OATP1B1 haplotype on pharmacokinetics of valsartan. Plasma concentration–time profiles of valsartan after oral administration of 40 mg valsartan in *OATP1B1*1a/*1a* subjects (*squares*, n = 5) and **1b/*1b* subjects (*inverted triangles*, n = 7) (**A**) and in **1a/*15* subjects (*triangles*, n = 6) and **1b/*15* subjects (*diamonds*, n = 5) (**B**). **C**, Box-whisker plot of AUC of valsartan in each haplotype group.

Table I. $AUC_{0\text{-}24}$ and CL_r of pravastatin and its metabolite (RMS-416), valsartan, and temocapril and its active metabolite (temocaprilat) in each haplotype group

	**1a/*1a (n = 5)*	**1b/*1b (n = 7)*	**1a/*15 (n = 6)*	**1b/*15 (n = 5)*
Pravastatin				
$AUC_{0\text{-}24}$ (ng · h/mL)	73.2 ± 23.5	47.4 ± 19.9†	69.2 ± 23.4	38.2 ± 15.9‡
CL_r (L/h)	15.1 ± 2.7	18.6 ± 7.6	12.6 ± 2.5	17.0 ± 3.5
Pravastatin plus RMS-416				
$AUC_{0\text{-}24}$ (ng · h/mL)	112 ± 25	76.1 ± 20.4	143 ± 40	95.1 ± 33.6‡
CL_r (L/h)	12.5 ± 2.0	16.0 ± 8.5	11.0 ± 1.5	13.5 ± 2.4
Valsartan				
$AUC_{0\text{-}24}$ (μg · h/mL)	12.3 ± 4.6	9.01 ± 3.33	9.40 ± 4.34	6.31 ± 3.64
CL_r (L/h)	0.450 ± 0.063	0.482 ± 0.049	0.489 ± 0.109	0.477 ± 0.096
Temocaprilat				
$AUC_{0\text{-}24}$ (ng · h/mL)	426 ± 91	371 ± 100	429 ± 41	389 ± 77
CL_r (L/h)	1.41 ± 0.06	1.29 ± 0.26	1.31 ± 0.12	1.32 ± 0.15
Temocapril				
$AUC_{0\text{-}24}$ (ng · h/mL)	18.5 ± 7.7	12.4 ± 4.1	19.0 ± 4.1	16.4 ± 5.0
CL_r (L/h)	0.818 ± 0.476	1.82 ± 1.16	1.21 ± 0.52	2.14 ± 1.77

Data are presented as mean ± SD.
$AUC_{0\text{-}24}$, Area under plasma concentration–time curve from 0 to 24 hours; CL_r, renal clearance.
†Significantly different from values in *1a/*1a subjects as determined by ANOVA with Fisher least significant difference test ($P < .05$).
‡Significantly different from values in *1a/*15 subjects as determined by ANOVA with Fisher least significant difference test ($P < .05$).

Effect of OATP1B1 haplotype on pharmacokinetics of temocapril and temocaprilat. After oral administration of temocapril, temocapril was rapidly eliminated from the blood, and the concentration of temocapril was undetectable at 1 to 2 hours after administration as a result of the rapid conversion of temocapril to the active metabolite temocaprilat by carboxylesterase. Temocaprilat was then detected at 0.25 hour, and its plasma concentration reached a maximum at 0.75 to 2 hours after intake of temocapril (Fig 3, *A* and *B*). The plasma concentration of

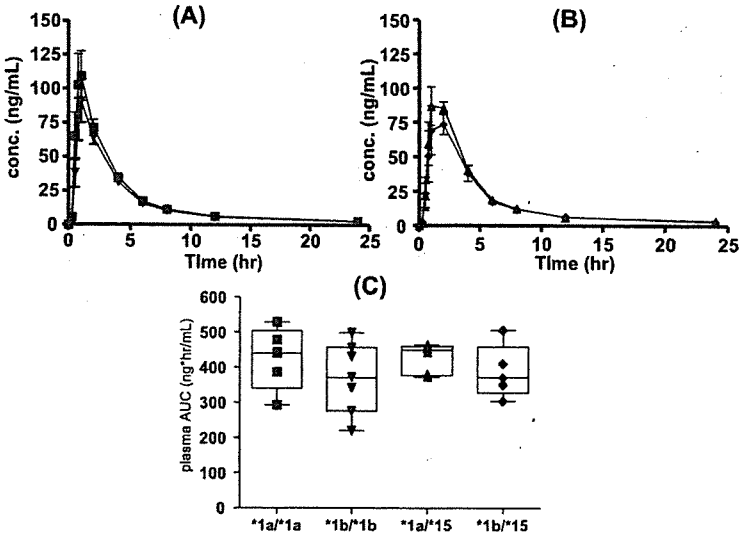

Fig 3. Effect of OATP1B1 haplotype on pharmacokinetics of temocaprilat. Plasma concentration–time profiles of temocaprilat after oral administration of 2 mg temocapril in *OATP1B1*1a/*1a* subjects (*squares*, n = 5) and **1b/*1b* subjects (*inverted triangles*, n = 7) (**A**) and in **1a/*15* subjects (*triangles*, n = 6) and **1b/*15* subjects (*diamonds*, n = 5) (**B**). **C**, Box-whisker plot of AUC of temocaprilat in each haplotype group.

temocaprilat showed a similar pattern in *OATP1B1*1b/*1b* and **1a/*1a* subjects (Fig 3, *A*) and **1b/*15* and **1a/*15* subjects (Fig 3, *B*). The mean $AUC_{0\text{-}24}$ of temocaprilat in **1b/*1b* subjects was not significantly very different from that in **1a/*1a* subjects (87% of **1a/*1a*), and the $AUC_{0\text{-}24}$ in **1b/*15* subjects was not different from that in **1a/*15* subjects (91% of **1a/*15*) (Fig 3, *C* and Table I). The *OATP1B1*15* allele did not affect the $AUC_{0\text{-}24}$ of temocaprilat. The CL_r of temocaprilat was almost the same in each haplotype group (Table I). On the other hand, the plasma concentration of temocapril in *OATP1B1*1b/*1b* subjects tended to be lower than that in **1a/*1a* subjects (Fig 4, *A*), and the plasma concentration in **1b/*15* subjects tended to be lower than that in **1a/*15* subjects (Fig 4, *B*). Although not statistically significant, the $AUC_{0\text{-}24}$ of temocapril in **1b/*1b* carriers was lower than that in **1a/*1a* carriers (67% of **1a/*1a*) and the $AUC_{0\text{-}24}$ in **1b/*15* carriers was lower than that in **1a/*15* carriers (86% of **1a/*15*) (Fig 4, *C*, and Table I), and the CL_r of temocapril in each haplotype group was not significantly different (Table I).

Correlation between AUC of pravastatin, valsartan, temocaprilat, and temocapril in each subject. The AUC values of valsartan in each subject were significantly correlated with those of pravastatin ($R = 0.630$, $P < .01$) (Fig 5, *A*). The AUC values of temocapril in each subject were also significantly correlated with those of pravastatin ($R = 0.602$, $P < .01$) (Fig 5, *C*). However, the AUC values of temocaprilat were not significantly correlated with those of pravastatin ($R = 0.229$) (Fig 5, *B*).

OATP1B1-mediated uptake of valsartan and temocaprilat in expression system. The time-dependent uptake of valsartan and temocaprilat in OATP1B1-expressing HEK293 cells was significantly higher than that in vector-transfected control cells (Fig 6).

OATP1B1-/MRP2-mediated transcellular of temocapril and RMS-416 in OATP1B1/MRP2 double-transfected MDCKII cells. As a positive control, we ascertained that the vectorial basal-to-apical transcellular transport of estradiol-17β-glucuronide (OATP1B1/MRP2 bisubstrate) was clearly observed in OATP1B1/MRP2 double-transfected cells (Fig 7, *C*), whereas symmetric transport was observed in OATP1B1 single-transfected cells and vector-transfected control cells (Fig 7, *A* and *B*) as shown in the previous report.[18] Under the same condition, basal-to-apical transport of temocapril and RMS-416 was significantly larger than that in the opposite direction in OATP1B1/MRP2 double-transfected cells (Fig 7, *F* and *I*), whereas their vectorial transport was not observed in OATP1B1 single-transfected cells (Fig 7, *E* and *H*) and vector-transfected control cells (Fig 7, *D* and *G*).

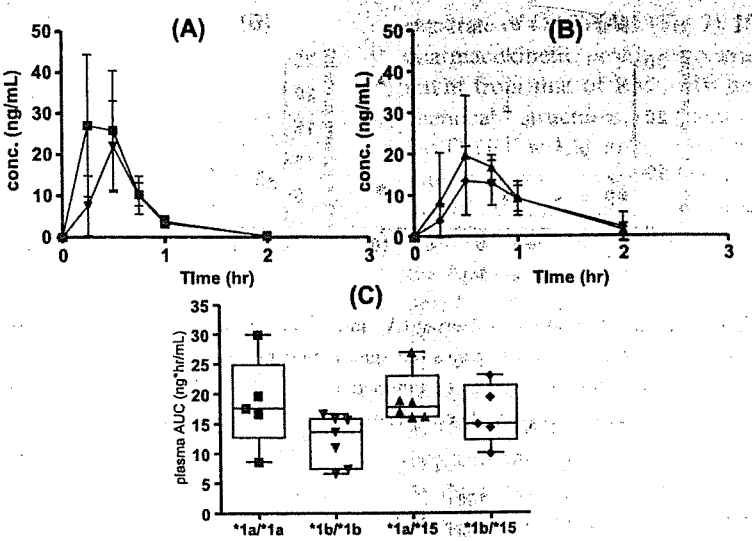

Fig 4. Effect of OATP1B1 haplotype on pharmacokinetics of temocapril. Plasma concentration–time profiles of temocapril after oral administration of 2 mg temocapril in *OATP1B1*1a/*1a* subjects (*squares*, n = 5) and **1b/*1b* subjects (*inverted triangles*, n = 7) (**A**) and in **1a/*15* subjects (*triangles*, n = 6) and **1b/*15* subjects (*diamonds*, n = 5) (**B**). **C**, Box-whisker plot of AUC of temocapril in each haplotype group.

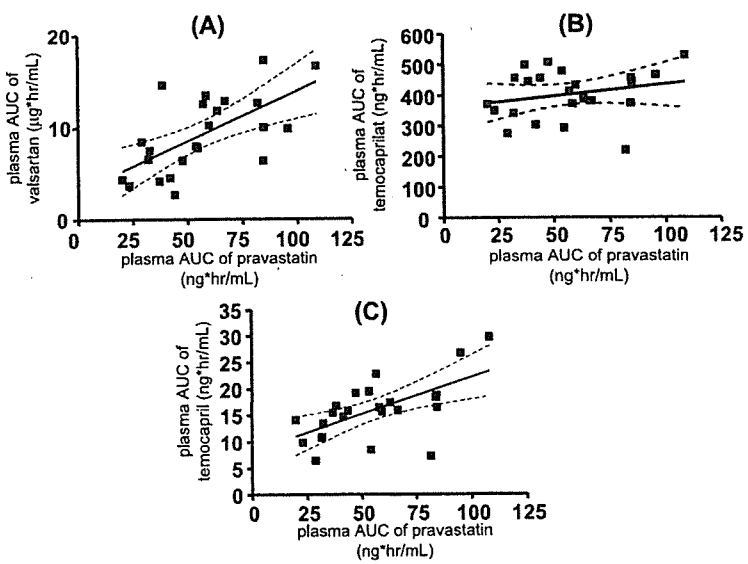

Fig 5. Correlation between AUC of pravastatin and valsartan (**A**), AUC of pravastatin and temocaprilat (**B**), and AUC of pravastatin and temocapril (**C**). Each *point* represents data for each subject. *Solid lines* represent fitted lines calculated by linear regression analysis, and *dotted lines* represent 95% confidence intervals of correlations.

DISCUSSION

We investigated the impact of the OATP1B1 haplotype, especially **1b*, on the pharmacokinetics of 3 anionic drugs, pravastatin, valsartan, and temocapril, in healthy volunteers. We also investigated whether the pharmacokinetics of each drug was correlated with that of other drugs in each subject.

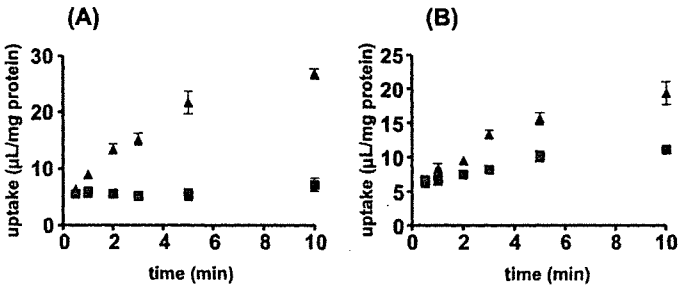

Fig 6. Time-dependent uptake of valsartan (**A**) and temocaprilat (**B**) in OATP1B1-expressing cells and control cells. The uptake of valsartan and temocaprilat by OATP1B1-transfected human embryonic kidney (HEK) 293 cells was examined at 37°C. *Triangles* and *squares* represent uptake by OATP1B1- and vector-transfected cells, respectively. Each *point* represents mean ± SE (n = 3).

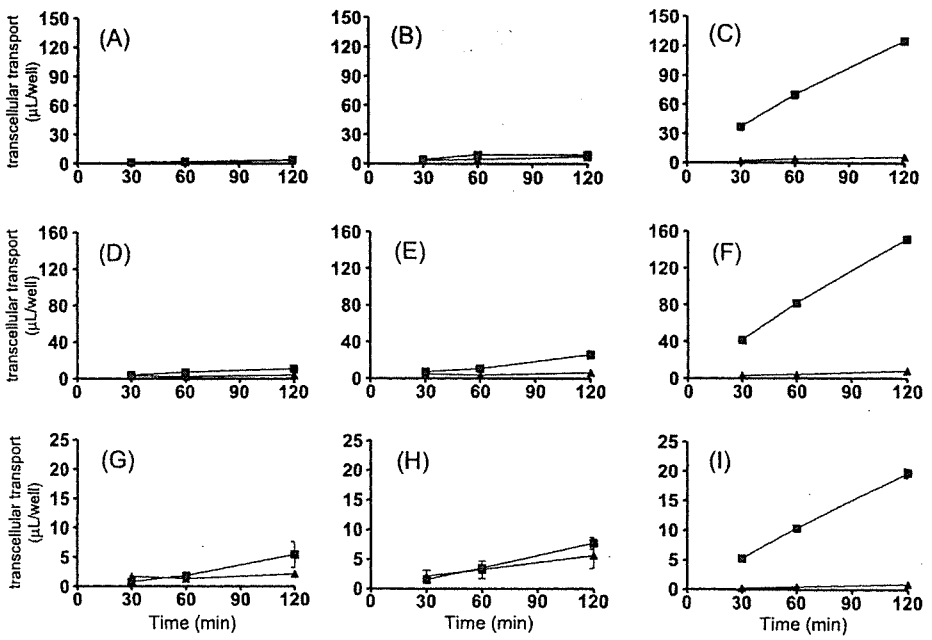

Fig 7. Time profiles for transcellular transport of estradiol-17β-glucuronide (**A**, **B**, and **C**), temocapril (**D**, **E**, and **F**), and RMS-416 (**G**, **H**, and **I**) across Madin-Darby canine kidney II (MDCKII) monolayers. Transcellular transport of estradiol-17β-glucuronide (1 μmol/L), temocapril (1 μmol/L), and RMS-416 (10 μmol/L) across MDCKII monolayers expressing OATP1B1 (**B**, **E**, and **H**) and both OATP1B1 and multidrug resistance associated protein 2 (MRP2) (**C**, **F**, and **I**) was compared with that across the control MDCKII monolayer (**A**, **D**, and **G**). *Triangles* and *squares* represent transcellular transport in apical-to-basal direction and basal-to-apical direction, respectively. Each *point* and *vertical bars* represent mean ± SE of 3 determinations. Where vertical bars are not shown, the SE was contained within the limits of the symbol.

Pravastatin, valsartan, and temocaprilat are mainly excreted into the bile without extensive metabolism, and the involvement of transporters is needed to explain their efficient accumulation in the liver. When the pharmacokinetic theory is considered, given the assumption that total clearance is accounted for by hepatic clearance, the AUC after oral administration of drugs (AUC_{oral}) can be expressed by equation 1:

$$AUC_{oral} = \frac{F \cdot Dose}{f_B \cdot CL_{int}} \quad (1)$$

in which F is the fraction of the dose absorbed into and through the gastrointestinal membranes, f_B is the blood unbound fraction, and CL_{int} is the hepatic intrinsic clearance. In addition, CL_{int} can be expressed by equation 2:

$$CL_{int} = CL_{uptake} \cdot \frac{CL_{ex} + CL_{metab}}{CL_{ex} + CL_{metab} + CL_{eff}} \quad (2)$$

where CL_{uptake}, CL_{ex}, CL_{metab}, and CL_{eff} represent the intrinsic clearances for hepatic uptake, biliary excretion, metabolism, and sinusoidal efflux, respectively.[6] When equations 1 and 2 are considered, CL_{uptake} directly affects the AUC after oral administration in any situation.

We especially focused on the impact of the *OATP1B1*1b* allele on the pharmacokinetics of the 3 drugs. The allele frequency of *OATP1B1*1b* is relatively high in some ethnic groups: 0.30 in white Americans, 0.74 in black Americans, and 0.63 in Japanese subjects.[9,10]

Pravastatin has been reported to be a substrate of OATP1B1.[1,8,18,20] We demonstrated that valsartan and temocaprilat could also be recognized by OATP1B1 as substrates (Fig 6).

The *OATP1B1*1b* allele significantly reduced the AUC of pravastatin compared with **1a*, which is consistent with a previous report.[12] The CL_r of pravastatin was not affected by **1b*, suggesting that the *OATP1B1*1b* variant apparently enhances the hepatic uptake activity of pravastatin. On the other hand, the *OATP1B1*15* allele did not remarkably affect the AUC of pravastatin in our study, which apparently differs from findings in earlier reports showing that the **15* allele results in a significant increase in the AUC of pravastatin.[10,11] After oral administration, a significant amount of pravastatin was converted to RMS-416 (3′α-isopravastatin), mainly in the stomach, by a chemical reaction rather than by enzymatic metabolism, because pravastatin is unstable in acidic solution.[21] In our study the interindividual difference in the AUC of RMS-416 was about 50-fold (2.37-120 ng · h/mL; mean, 48.8 ng · h/mL). It is generally accepted that the pH values in the stomach exhibit large interindividual differences. We hypothesized that these differences might affect the conversion rate to RMS-416, which could mask the effect of *OATP1B1*15* on the pharmacokinetics of pravastatin in our cases. RMS-416 is an epimer of pravastatin, and only the position of 1 hydroxyl group was different. We confirmed that RMS-416 is also a substrate of OATP1B1 (Fig 7). If it is assumed that the pharmacokinetic profile of pravastatin was not so different from that of RMS-416 because of their similar chemical structures, a genetic polymorphism of OATP1B1 would affect the pharmacokinetics of the sum of pravastatin and RMS-416 more markedly than that of pravastatin itself. In our study we could see the expected tendency showing that the **1b* allele reduced the AUC of the sum of pravastatin and RMS-416 compared with **1a*, whereas the **15* allele increased the AUC (Table I). Recent studies have demonstrated that the Val174Ala mutation in OATP1B1 could alter the cholesterol-lowering effect of pravastatin.[22,23] Because RMS-416 is not pharmacologically active, our study suggests that the conversion rate to RMS-416, as well as the genetic polymorphism in OATP1B1, may have an effect on the pharmacokinetics and pharmacologic action of pravastatin.

In the case of valsartan the **1b* allele showed a reduction in the AUC of valsartan, but the **15* allele did not show any increase in the AUC, which is almost the same as pravastatin. Unfortunately, the difference in its AUC between **1a* and **1b* did not show statistical significance, probably because of the lack of statistical power, and we believe that a greater number of subjects will be needed to show the significant difference. Valsartan was partly metabolized to the 4-hydroxylated form (M-2) by CYP2C9,[24] but a previous report indicated that, after oral administration of [^{14}C]-valsartan, this metabolite accounted for only 10% of the total radioactivity in the feces and urine.[24] Therefore the interindividual difference in CYP2C9 activity plays only a minor role in the pharmacokinetics of valsartan. The solubility of valsartan is drastically affected by the pH, and it is possible that an interindividual difference in the pH value in the gastrointestinal tract may affect its solubility and the subsequent amount of valsartan absorbed.[25] However, 1 report demonstrated that coadministration of cimetidine increased the AUC only by 7%.[26] Thus the exact reason why the **15* allele did not affect the pharmacokinetics of valsartan remains to be clarified.

The AUC of temocapril and temocaprilat was not changed significantly in each haplotype group. However, there was a trend suggesting that the **1b* allele reduced the AUC of temocapril and temocaprilat and that the **15* allele showed a slight increase in the AUC. We determined that temocapril is also a substrate of OATP1B1 (Fig 7). The difference in the AUC of temocaprilat in each haplotype group was relatively small compared with that of the other drugs.

We also compared the pharmacokinetics of the 3 drugs in each subject, and the AUC of pravastatin was

significantly correlated with that of valsartan and temocapril, but not temocaprilat (Fig 5). This result suggested that the clearance mechanism of pravastatin may be shared with that of valsartan and temocapril and that the relative contribution of OATP1B1 to the hepatic uptake of pravastatin may be similar to that of valsartan and temocapril but larger than that of temocaprilat.

Some in vitro studies have indicated that the transport activity of several compounds including pravastatin in the *OATP1B1*1b* variant was almost comparable to that of *OATP1B1*1a*.[7–9,27] However, this study demonstrated that *OATP1B1*1b* subjects showed an increase in hepatic clearance compared with that of *OATP1B1*1a* subjects. We hypothesized that this apparent discrepancy may be explained by the higher expression level of *OATP1B1*1b* in the liver compared with that of *OATP1B1*1a*. This can be proven by investigating the relative expression level of *OATP1B1*1a* and **1b* in several batches of human hepatocytes that are genotyped in advance. Moreover, we must pay attention to several pharmacokinetic issues such as the different proportion of hepatic clearance to total clearance, the different contribution of OATP1B1 to overall hepatic uptake, and the substrate specificity of the effect of genetic polymorphisms in OATP1B1. The percentage of hepatic clearance with regard to total clearance has been estimated to be about 53% for pravastatin, 71% for valsartan, and 62% for temocaprilat in humans[24,28] (drug information for temocaprilat provided by Sankyo). Previous reports suggest that the de-esterification of temocapril mainly occurs in the liver (drug information published by Sankyo). The urinary excretion of temocapril as a percentage of the administered dose is about 1.1% in this study. We believe that it is possible that temocapril is efficiently taken up into hepatocytes, followed by conversion to temocaprilat, and its hepatic clearance is much higher than its CL_r. That may be the reason why the AUC of temocapril showed a better correlation with that of pravastatin than with that of temocaprilat. Regarding the contribution of individual transporters, our preliminary study suggested that all 3 compounds are substrates of OATP1B3, as well as OATP1B1 (Hirano M, Maeda K, Sugiyama Y, unpublished data, Aug 25, 2004). The previous studies suggested that pravastatin is thought to be mainly taken up via OATP1B1.[20] From the result of the present study, we speculated that the relative importance of OATP1B1 with regard to hepatic clearance is in the following order: pravastatin greater than valsartan and temocapril greater than temocaprilat. We have established the method for estimating the contribution of OATP1B1 and OATP1B3 to overall hepatic uptake by using expression systems and human hepatocytes.[5] With this information being taken into consideration, the prediction of the effect of genetic polymorphisms in OATP1B1 on the pharmacokinetics of drugs from in vitro data will be the subject of further investigation.

In conclusion, our study indicated that the *OATP1B1*1b* allele increases the hepatic clearance of pravastatin compared with that of the **1a* allele, and valsartan and temocapril showed a similar tendency. In addition, the AUC of pravastatin correlates well with that of valsartan and temocapril, suggesting that pravastatin, valsartan, and temocapril may share the same elimination pathway.

We thank Sankyo for providing Mevalotin tablets, Acecol tablets, [^{14}C]-labeled and unlabeled temocaprilat, temocapril, RMS-416, and R-122798 and Novartis Pharma for providing Diovan tablets and tritium-labeled and unlabeled valsartan. We are grateful to Dr Kiyoshi Kawabata (Sankyo) for teaching us the method for the quantification of pravastatin, RMS-416, temocapril, and temocaprilat. We are also grateful to Drs Ryosei Kawai and Yuko Tsukamoto, Novartis Pharma, and Drs Toshihiko Ikeda, Yasushi Orihashi, and Hideo Naganuma, Sankyo, for supporting our study and giving us helpful suggestions.

The authors have no conflict of interest.

References

1. Hsiang B, Zhu Y, Wang Z, Wu Y, Sasseville V, Yang WP, et al. A novel human hepatic organic anion transporting polypeptide (OATP2). Identification of a liver-specific human organic anion transporting polypeptide and identification of rat and human hydroxymethylglutaryl-CoA reductase inhibitor transporters. J Biol Chem 1999;274:37161-8.
2. Abe T, Kakyo M, Tokui T, Nakagomi R, Nishio T, Nakai D, et al. Identification of a novel gene family encoding human liver-specific organic anion transporter LST-1. J Biol Chem 1999;274:17159-63.
3. Konig J, Cui Y, Nies AT, Keppler D. A novel human organic anion transporting polypeptide localized to the basolateral hepatocyte membrane. Am J Physiol Gastrointest Liver Physiol 2000;278:G156-64.
4. Shitara Y, Itoh T, Sato H, Li AP, Sugiyama Y. Inhibition of transporter-mediated hepatic uptake as a mechanism for drug-drug interaction between cerivastatin and cyclosporin A. J Pharmacol Exp Ther 2003;304:610-6.
5. Hirano M, Maeda K, Shitara Y, Sugiyama Y. Contribution of OATP2 (OATP1B1) and OATP8 (OATP1B3) to the hepatic uptake of pitavastatin in humans. J Pharmacol Exp Ther 2004;311:139-46.
6. Shitara Y, Sato H, Sugiyama Y. Evaluation of drug-drug interaction in the hepatobiliary and renal transport of drugs. Annu Rev Pharmacol Toxicol 2005;45:689-723.
7. Iwai M, Suzuki H, Ieiri I, Otsubo K, Sugiyama Y. Functional analysis of single nucleotide polymorphisms of

hepatic organic anion transporter OATP1B1 (OATP-C). Pharmacogenetics 2004;14:749-57.
8. Kameyama Y, Yamashita K, Kobayashi K, Hosokawa M, Chiba K. Functional characterization of SLCO1B1 (OATP-C) variants, SLCO1B1*5, SLCO1B1*15 and SLCO1B1*15+C1007G, by using transient expression systems of HeLa and HEK293 cells. Pharmacogenet Genomics 2005;15:513-22.
9. Tirona RG, Leake BF, Merino G, Kim RB. Polymorphisms in OATP-C: identification of multiple allelic variants associated with altered transport activity among European- and African-Americans. J Biol Chem 2001;276:35669-75.
10. Nishizato Y, Ieiri I, Suzuki H, Kimura M, Kawabata K, Hirota T, et al. Polymorphisms of OATP-C (SLC21A6) and OAT3 (SLC22A8) genes: consequences for pravastatin pharmacokinetics. Clin Pharmacol Ther 2003;73:554-65.
11. Niemi M, Schaeffeler E, Lang T, Fromm MF, Neuvonen M, Kyrklund C, et al. High plasma pravastatin concentrations are associated with single nucleotide polymorphisms and haplotypes of organic anion transporting polypeptide-C (OATP-C, SLCO1B1). Pharmacogenetics 2004;14:429-40.
12. Mwinyi J, Johne A, Bauer S, Roots I, Gerloff T. Evidence for inverse effects of OATP-C (SLC21A6) 5 and 1b haplotypes on pravastatin kinetics. Clin Pharmacol Ther 2004;75:415-21.
13. Niemi M, Backman JT, Kajosaari LI, Leathart JB, Neuvonen M, Daly AK, et al. Polymorphic organic anion transporting polypeptide 1B1 is a major determinant of repaglinide pharmacokinetics. Clin Pharmacol Ther 2005;77:468-78.
14. Niemi M, Kivisto KT, Hofmann U, Schwab M, Eichelbaum M, Fromm MF. Fexofenadine pharmacokinetics are associated with a polymorphism of the SLCO1B1 gene (encoding OATP1B1). Br J Clin Pharmacol 2005;59:602-4.
15. Israili ZH. Clinical pharmacokinetics of angiotensin II (AT1) receptor blockers in hypertension. J Hum Hypertens 2000;14(Suppl 1):S73-86.
16. Oizumi K, Koike H, Sada T, Miyamoto M, Nishino H, Matsushita Y, et al. Pharmacological profiles of CS-622, a novel angiotensin converting enzyme inhibitor. Jpn J Pharmacol 1988;48:349-56.
17. Ishizuka H, Konno K, Naganuma H, Sasahara K, Kawahara Y, Niinuma K, et al. Temocaprilat, a novel angiotensin-converting enzyme inhibitor, is excreted in bile via an ATP-dependent active transporter (cMOAT) that is deficient in Eisai hyperbilirubinemic mutant rats (EHBR). J Pharmacol Exp Ther 1997;280:1304-11.
18. Sasaki M, Suzuki H, Ito K, Abe T, Sugiyama Y. Transcellular transport of organic anions across a double-transfected Madin-Darby canine kidney II cell monolayer expressing both human organic anion-transporting polypeptide (OATP2/SLC21A6) and multidrug resistance-associated protein 2 (MRP2/ABCC2). J Biol Chem 2002;277:6497-503.
18a. Lowry OH, Rosebrough NJ, Farr AL, Randall RJ. Protein measurement with the Folin phenol reagent. J Biol Chem 1951;193:265-75.
19. Kawabata K, Sanata N, Urasaki Y. Quantitative determination of pravastatin and R-416, its main metabolite in human plasma, by liquid chromatography-tandem mass spectrometry. J Chromatogr B Analyt Technol Biomed Life Sci 2005;816:73-9.
20. Nakai D, Nakagomi R, Furuta Y, Tokui T, Abe T, Ikeda T, et al. Human liver-specific organic anion transporter, LST-1, mediates uptake of pravastatin by human hepatocytes. J Pharmacol Exp Ther 2001;297:861-7.
21. Triscari J, O'Donnell D, Zinny M, Pan HY. Gastrointestinal absorption of pravastatin in healthy subjects. J Clin Pharmacol 1995;35:142-4.
22. Tachibana-Iimori R, Tabara Y, Kusuhara H, Kohara K, Kawamoto R, Nakura J, et al. Effect of genetic polymorphism of OATP-C (SLCO1B1) on lipid-lowering response to HMG-CoA reductase inhibitors. Drug Metab Pharmacokinet 2004;19:375-80.
23. Niemi M, Neuvonen PJ, Hofmann U, Backman JT, Schwab M, Lutjohann D, et al. Acute effects of pravastatin on cholesterol synthesis are associated with SLCO1B1 (encoding OATP1B1) haplotype *17. Pharmacogenet Genomics 2005;15:303-9.
24. Waldmeier F, Flesch G, Muller P, Winkler T, Kriemler HP, Buhlmayer P, et al. Pharmacokinetics, disposition and biotransformation of [14C]-radiolabelled valsartan in healthy male volunteers after a single oral dose. Xenobiotica 1997;27:59-71.
25. Criscione L, Bradley W, Buhlmayer P, Whitebread S, Glazer R, Lloyd P, et al. Valsartan: pre-clinical and clinical profile of an antihypertensive angiotensin-II antagonist. Cardiovasc Drug Rev 1995;13:230-50.
26. Schmidt EK, Antonin KH, Flesch G, Racine-Poon A. An interaction study with cimetidine and the new angiotensin II antagonist valsartan. Eur J Clin Pharmacol 1998;53:451-8.
27. Nozawa T, Minami H, Sugiura S, Tsuji A, Tamai I. Role of organic anion transporter OATP1B1 (OATP-C) in hepatic uptake of irinotecan and its active metabolite, 7-ethyl-10-hydroxycamptothecin: in vitro evidence and effect of single nucleotide polymorphisms. Drug Metab Dispos 2005;33:434-9.
28. Singhvi SM, Pan HY, Morrison RA, Willard DA. Disposition of pravastatin sodium, a tissue-selective HMG-CoA reductase inhibitor, in healthy subjects. Br J Clin Pharmacol 1990;29:239-43.

0090-9556/07/3501-72–78$20.00
DRUG METABOLISM AND DISPOSITION
Vol. 35, No. 1
12088/3160040
Printed in U.S.A.

DMD 35:72–78, 2007

Identification of Human Cytochrome P450 Isozymes Involved in Diphenhydramine *N*-Demethylation

Tomoko Akutsu, Kaoru Kobayashi, Koichi Sakurada, Hiroshi Ikegaya, Tomomi Furihata, and Kan Chiba

Laboratory of Pharmacology and Toxicology, Graduate School of Pharmaceutical Sciences, Chiba University, Chiba-shi, Chiba, Japan (T.A., K.K., T.F., K.C.); and Third Biology Section, Department of First Forensic Science, National Research Institute of Police Science, Kashiwa-shi, Chiba, Japan (T.A., K.S., H.I.)

Received July 17, 2006; accepted September 29, 2006

ABSTRACT:

Diphenhydramine is widely used as an over-the-counter antihistamine. However, the specific human cytochrome P450 (P450) isozymes that mediate the metabolism of diphenhydramine in the range of clinically relevant concentrations (0.14–0.77 μM) remain unclear. Therefore, P450 isozymes involved in *N*-demethylation, a main metabolic pathway of diphenhydramine, were identified by a liquid chromatography-mass spectrometry method developed in our laboratory. Among 14 recombinant P450 isozymes, CYP2D6 showed the highest activity of diphenhydramine *N*-demethylation (0.69 pmol/min/pmol P450) at 0.5 μM. CYP2D6 catalyzed diphenhydramine *N*-demethylation as a high-affinity P450 isozyme, the K_m value of which was 1.12 ± 0.21 μM. In addition, CYP1A2, CYP2C9, and CYP2C19 were identified as low-affinity components. In human liver microsomes, involvement of CYP2D6, CYP1A2, CYP2C9, and CYP2C19 in diphenhydramine *N*-demethylation was confirmed by using P450 isozyme-specific inhibitors. In addition, contributions of these P450 isozymes estimated by the relative activity factor were in good agreement with the results of inhibition studies. Although an inhibitory effect of diphenhydramine on the metabolic activity of CYP2D6 has been reported previously, the results of the present study suggest that it is not only a potent inhibitor but also a high-affinity substrate of CYP2D6. Therefore, it is worth mentioning that the sedative effect of diphenhydramine might be caused by coadministration of CYP2D6 substrate(s)/inhibitor(s). In addition, large differences in the metabolic activities of CYP2D6 and those of CYP1A2, CYP2C9, and CYP2C19 could cause the individual differences in anti-allergic efficacy and the sedative effect of diphenhydramine.

Histamine H1 receptor antagonists (antihistamines) are useful in the treatment of various allergic diseases such as allergic rhinitis, conjunctivitis, atopic dermatitis, urticaria, asthma, and anaphylaxis (Mizushima, 2006). Recently, there has been increasing interest in the metabolism and pharmacodynamic effects of classic antihistamines because of severe deleterious cytochrome P450 (P450)-based drug-drug interactions observed with second-generation antihistamines such as terfenadine (Monahan et al., 1990; Paakkari, 2002). Diphenhydramine is a first-generation antihistamine synthesized in the 1940s (Loew et al., 1946) and has been widely used as an over-the-counter drug (Kay and Quig, 2001; Food and Drug Administration, 2002). Since this antihistamine is available without prescription, it is possible that it is taken with various drugs, so that an interaction may occur when the same P450 isozyme(s) is involved in the major metabolic processes of diphenhydramine and concomitant drug(s).

Diphenhydramine is extensively metabolized by demethylation to *N*-demethyl diphenhydramine, followed by rapid demethylation to *N*,*N*-didemethyl diphenhydramine. *N*,*N*-Didemethyl diphenhydramine is further metabolized by oxidative deamination to diphenylmethoxyacetic acid. These metabolic pathways are thought to be major pathways in humans (Chang et al., 1974; Blyden et al., 1986), although little is known about the enzymes involved in these metabolic pathways of diphenhydramine because of the limited requirements for pharmacokinetics/metabolism data before marketing classic antihistamines. However, the metabolism of classic antihistamines seems to be mediated by CYP2D6 because of the similar structural characteristics of many CYP2D6 substrates and inhibitors (Koymans et al., 1992; Smith and Jones, 1992; de Groot et al., 1997). In fact, several classic antihistamines, such as chlorpheniramine, mequitazine, and promethazine, have been shown to be metabolized by CYP2D6 (Nakamura et al., 1996, 1998; Yasuda et al., 2001). In addition, previous studies revealed that diphenhydramine inhibited the metabolism of several CYP2D6 substrates in vivo and in vitro (Hamelin et al., 1998, 2000; Lessard et al., 2001; He et al., 2002). These findings suggest that the metabolism of diphenhydramine is also mediated by CYP2D6.

However, Lessard et al. (2001) reported that the clearance of diphenhydramine to its *N*-demethylated metabolite (2-benzhydryloxy-*N*-methyl-ethanamine) is not different in extensive and poor metabolizer phenotypes of CYP2D6 and suggested that diphenhydramine is not extensively metabolized by this P450 isozyme. In addition, multiple P450 isozymes, CYP1A2, CYP2C18, CYP2C19, CYP2D6, and CYP2B6, have been reported to be involved in the *N*-demethylation of diphenhydramine at 20 μM (Hamelin et al., 2001; Sharma and Hame-

Article, publication date, and citation information can be found at http://dmd.aspetjournals.org.
doi:10.1124/dmd.106.012088.

ABBREVIATIONS: P450, cytochrome P450; LC/MS, liquid chromatography/mass spectrometry; RAF, relative activity factor; SKF-525A, proadifen.

lin, 2003). Nonetheless, it remains unclear whether these P450 isozymes also catalyze the *N*-demethylation of diphenhydramine at clinically relevant concentrations, which are 37 to 83 ng/ml (0.14–0.33 μM) in plasma after oral administration, and 99 to 196 ng/ml (0.38–0.77 μM) in plasma after intravenous injection of 50 mg of diphenhydramine hydrochloride (Carruthers et al., 1978; Blyden et al., 1986).

Therefore, the aim of this study was to identify the P450 isozymes involved in *N*-demethylation of diphenhydramine using recombinant P450 isozymes and human liver microsomes at a clinically relevant concentration (0.5 μM) of diphenhydramine by a liquid chromatography-mass spectrometry (LC/MS) method developed in our laboratory. Contributions of multiple P450 isozymes to human liver microsomal *N*-demethylation of diphenhydramine were also estimated by application of the relative activity factor (RAF) (Crespi, 1995) and were verified by the results of inhibition studies using P450 isozyme-specific inhibitors.

Materials and Methods

Chemicals and Reagents. Diphenhydramine hydrochloride, quinidine sulfate, furafylline, sulfaphenazole, and omeprazole were purchased from Sigma (St. Louis, MO). Orphenadrine hydrochloride was purchased from MP Biomedicals (Irvine, CA). SKF-525A was purchased from Toronto Research Chemicals (North York, ON, Canada). Glucose 6-phosphate, glucose-6-phosphate dehydrogenase, and $NADP^+$ were purchased from Oriental Yeast Co. (Tokyo, Japan). 2-Benzhydryloxy-*N*-methyl-ethanamine (*N*-demethyl diphenhydramine) was synthesized by Wako Pure Chemical Industries (Osaka, Japan). Human liver microsomes (HG3, 6, 23, 30, 42, 43, 56, 66, 70, 89, 93, 112, and pooled) and microsomes prepared from baculovirus-infected insect cells expressing CYP1A1, CYP1A2, CYP2A6, CYP2B6, CYP2C8, CYP2C9, CYP2C18, CYP2C19, CYP2D6, CYP2E1, CYP3A4, and CYP4A11 individually were obtained from BD Gentest (Woburn, MA). All recombinant P450s had been coexpressed with NADPH P450 oxidoreductase. Recombinant CYP2A6, CYP2B6, CYP2C8, CYP2C9, CYP2C19, CYP2E1, and CYP3A4 were also coexpressed with cytochrome b_5. Microsomal protein expressing NADPH P450 oxidoreductase and cytochrome b_5 was used as a control. Other chemicals and reagents used in this study were research-grade purchased from Wako.

Diphenhydramine *N*-Demethylation Assay. The basic incubation mixture contained recombinant P450 isozyme (5 pmol of P450/ml) or human liver microsomes (0.1 mg/ml), 0.1 mM EDTA, 100 mM potassium phosphate buffer (pH 7.4), and 0.5 μM diphenhydramine in a final incubation volume of 250 μl. The reaction was initiated by the addition of an NADPH-generating system (0.5 mM $NADP^+$, 2.0 mM glucose 6-phosphate, 1 U/ml glucose-6-phosphate dehydrogenase, and 4 mM $MgCl_2$). Incubation was performed for 20 min for recombinant P450 isozyme or 60 min for human liver microsomes at 37°C and terminated by the addition of 250 μl of 0.1 M HCl. Orphenadrine was added as an internal standard at a final concentration of 0.2 μM. The reaction was performed in a linear range with respect to the protein concentration and the incubation time for each recombinant P450 isozyme and pooled human liver microsomes. Under the incubation conditions of the present study, negligible metabolism of *N*-demethyl diphenhydramine to *N,N*-didemethyl diphenhydramine was confirmed by single ion monitoring at *m/z* 228, using the pseudomolecular ion of *N,N*-didemethyl diphenhydramine. For calibration standards, incubation was performed without diphenhydramine and terminated by the addition of 250 μl of 0.1 M HCl. Then, *N*-demethyl diphenhydramine was added to the reaction mixture at final concentrations of 5 nM to 5 μM. The correlation coefficient (r) for the calibration curve calculated by the least-squares regression method was $r > 0.99$ at final concentrations of 5 nM to 5 μM. The coefficient of variation for the assay in the present study was 9.7% ($n = 5$). All procedures were performed in siliconized glass tubes to avoid adsorption of the microsomes, substrate, and metabolites.

Solid-Phase Extraction. Solid-phase extraction was performed by the method of Miyaguchi et al. (2006) with slight modifications. The incubation mixture was applied to a mix-mode solid-phase extraction cartridge (Oasis MCX cartridge; Waters, Milford, MA). The cartridge was conditioned with 1 ml each of acetonitrile and distilled water before use. After application of the reaction mixture, the cartridge was washed with 1 ml each of 0.1 M HCl and acetonitrile and then eluted with 1 ml of 5% ammonium hydroxide in acetonitrile. In this solid-phase extraction method, lipophilic basic compounds were selectively eluted. The eluate was dried under a gentle stream of nitrogen at 45°C and reconstituted by 100 μl of distilled water/acetonitrile (50:50 v/v). Ten microliters of the reconstituted sample was applied to an LC/MS system. In this extraction procedure, the recovery rates of *N*-demethyl diphenhydramine were calculated by three or four independent analyses to be 100.0 ± 2.2% at 50 nM and 95.0 ± 2.2% at 5 μM. Coefficients of variation of this solid-phase extraction method were 2.2% at 50 nM and 2.3% at 5 μM.

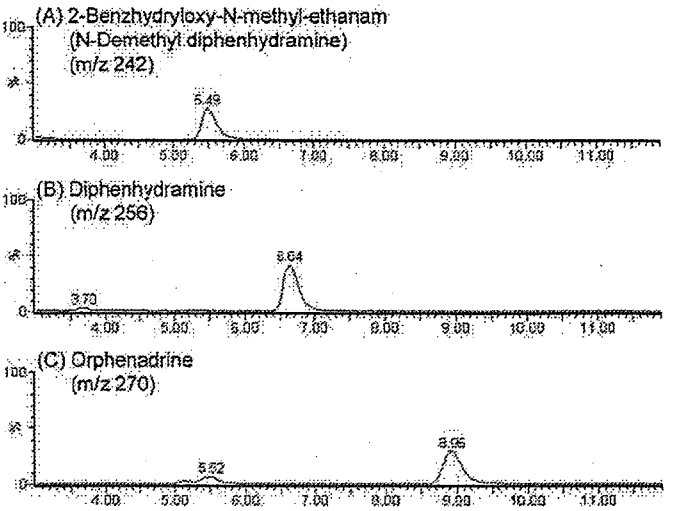

FIG. 1. Mass chromatograms of 2-benzhydryloxy-*N*-methyl-ethanamine (*N*-demethyl diphenhydramine) (A), diphenhydramine (B), and orphenadrine derived from an incubation mixture of human liver microsomes (C). Pseudomolecular ions of *N*-demethyl diphenhydramine, diphenhydramine, and orphenadrine were monitored at *m/z* 242, 256, and 270, respectively. The retention times of *N*-demethyl diphenhydramine, diphenhydramine, and orphenadrine in this analytical condition were 5.5, 6.6, and 9.0 min, respectively.

LC/MS Conditions. Determination of diphenhydramine and its *N*-demethylated metabolite was carried out using an LC/MS system. The LC system consisted of an Alliance 2695 separation module (Waters) and an XTerra MS C18 column (particle size of 3.5 μm, 2.1 mm i.d. × 100 mm; Waters). The mobile phase consisted of 0.1% ammonia in water/acetonitrile (50:50 v/v) at a flow rate of 0.25 ml/min. The column temperature was maintained at 40°C. This LC system was connected to an ion trap MS system (Micromass ZQ; Waters) with an electron spray ionization probe. The compounds were detected in the positive-ion electron spray ionization mode. For maximal sensitivity, the ion source temperature and cone voltage were optimized at 120°C and 20 V, respectively. Nitrogen was used for desolvation at a flow rate of 500 l/h. The desolvation temperature was 350°C. For quantitation, monitoring of single ions was performed at *m/z* of pseudomolecular ions of *N*-demethyl diphenhydramine (*m/z* 242), diphenhydramine (*m/z* 256), and orphenadrine (*m/z* 270). *N*-Demethyl diphenhydramine, diphenhydramine, and orphenadrine were identified by matching the retention time and *m/z* of pseudomolecular ions with those of authentic materials. The retention times of *N*-demethyl diphenhydramine, diphenhydramine, and orphenadrine in this analytical condition were 5.5 min, 6.6 min, and 9.0 min, respectively (Fig. 1). Limits of quantification in the assays with recombinant P450s and with human liver microsomes are final concentrations of 2.0 nM and 2.8 nM, respectively, calculated as signal-to-noise ratios of more than 10.

Kinetics of Diphenhydramine *N*-Demethylation in Pooled Human Liver Microsomes. Kinetics of diphenhydramine *N*-demethylation in pooled human liver microsomes were determined from formation rates of *N*-demethyl diphenhydramine at diphenhydramine concentrations ranging from 0.5 to 500 μM. Involvement of multiple enzymes was assessed by Eadie-Hofstee plots. When the Eadie-Hofstee plot was not linear, the kinetic parameters of high- and low-affinity components (K_{m1} and V_{max1} for the high-affinity component and K_{m2} and V_{max2} for the low-affinity component) were estimated by graphic

analysis of the two-component Michaelis-Menten model calculated by using DeltaGraph 4.5 (Nippon Polaroid, Tokyo, Japan).

Correlation Study. Correlation coefficients between diphenhydramine *N*-demethylation activity at 0.5 μM and other P450 isozyme-specific activities were calculated in human liver microsomes from 12 individual donors. Data of activities of phenacetin *O*-deethylation for CYP1A2, coumarin 7-hydroxylation for CYP2A6, (*S*)-mephenytoin *N*-demethylation for CYP2B6, paclitaxel 6α-hydroxylation for CYP2C8, diclofenac 4′-hydroxylation for CYP2C9, (*S*)-mephenytoin 4′-hydroxylation for CYP2C19, bufuralol 1′-hydroxylation for CYP2D6, chlorzoxazone 6-hydroxylation for CYP2E1, testosterone 6β-hydroxylation for CYP3A4, and lauric acid 12-hydroxylation for CYP4A were provided by BD Gentest.

Chemical Inhibition Study. The effects of P450 isozyme-specific inhibitors on diphenhydramine *N*-demethylation activity were investigated in human liver microsomes. Human liver microsomal protein (0.1 mg/ml) was incubated with 0.5 μM diphenhydramine in the presence of 1 μM quinidine (a selective CYP2D6 inhibitor) at 37°C for 60 min. Correlation coefficients between the residual diphenhydramine *N*-demethylation activity in the presence of 1 μM quinidine and other P450 isozyme-specific activities were calculated in human liver microsomes from 12 individual donors. Inhibition studies with 10 μM furafylline for CYP1A2, 10 μM sulfaphenazole for CYP2C9, and 10 μM omeprazole for CYP2C19 in individual human liver microsomes HG30, HG66, HG89, and HG112 and in pooled human liver microsomes were also performed. These human liver microsomes from individual donors were selected because they showed characteristic activities of CYP2D6, CYP1A2, CYP2C9, and CYP2C19 and comparable activities of diphenhydramine *N*-demethylation. The concentrations of specific inhibitors were verified by inhibition of the specific activities of corresponding P450 isozymes in human liver microsomes (Bourrie et al., 1996; Kobayashi et al., 1999; Giraud et al., 2004).

Kinetics of Diphenhydramine *N*-Demethylation in Recombinant P450 Isozymes. Kinetics of diphenhydramine *N*-demethylation in recombinant CYP1A2, CYP2C9, CYP2C19, and CYP2D6 were determined from formation rates of *N*-demethyl diphenhydramine at diphenhydramine concentrations ranging from 0.05 to 20 μM for CYP2D6 and from 0.5 to 500 μM for CYP1A2, CYP2C9, and CYP2C19. The kinetic parameters (K_m, V_{max}, and V_{max}/K_m) were estimated by graphic analysis of the one-component Michaelis-Menten model calculated by using DeltaGraph 4.5.

Contribution of Each P450 Isozyme to Diphenhydramine *N*-Demethylation in Human Liver Microsomes. The percentage contribution of each P450 isozyme to diphenhydramine *N*-demethylation in human liver microsomes was estimated by application of the RAF (Crespi, 1995). The RAF for CYP1A2 was determined as the ratio of the activity of phenacetin *O*-deethylation, a specific metabolic reaction of CYP1A2, in human liver microsomes to that of recombinant CYP1A2. Similarly, diclofenac 4′-hydroxylation, (*S*)-mephenytoin 4′-hydroxylation, and bufuralol 1′-hydroxylation were used for calculations of the RAFs of CYP2C9, CYP2C19, and CYP2D6, respectively. The clearance of each P450 isozyme in human liver microsomes is represented by the clearance of each recombinant P450 isozyme multiplied by the RAF. Clearances of human liver microsomes are shown as the sum of the clearances of P450 isozymes in human liver microsomes. The contribution of each P450 isozyme to diphenhydramine *N*-demethylation in human liver microsomes is represented by the percentage of clearance of human liver microsomes. The percentages of contribution of P450 isozymes to diphenhydramine *N*-demethylation in human liver microsomes estimated by application of the RAF were compared with the percentages of inhibition by P450 isozyme-specific inhibitors.

Results

Diphenhydramine *N*-Demethylation Activity in Recombinant P450 Isozymes. Diphenhydramine *N*-demethylation activities at 0.5 μM in microsomes of baculovirus-infected insect cells expressing 14 individual P450 isozymes were determined (Fig. 2). CYP2D6 showed the highest activity of diphenhydramine *N*-demethylation (0.69 pmol/min/pmol P450). The activity of recombinant CYP2C19 was 0.071 pmol/min/pmol P450, the second highest. Recombinant CYP1A2, CYP2B6, and CYP2C18 also showed diphenhydramine *N*-demethylation activities (0.043, 0.023, and 0.036 pmol/min/pmol P450, respectively), whereas CYP1A1, CYP2C9, and CYP3A4 showed detectable but low activity (0.010, 0.0082, and 0.0084 pmol/min/pmol P450, respectively).

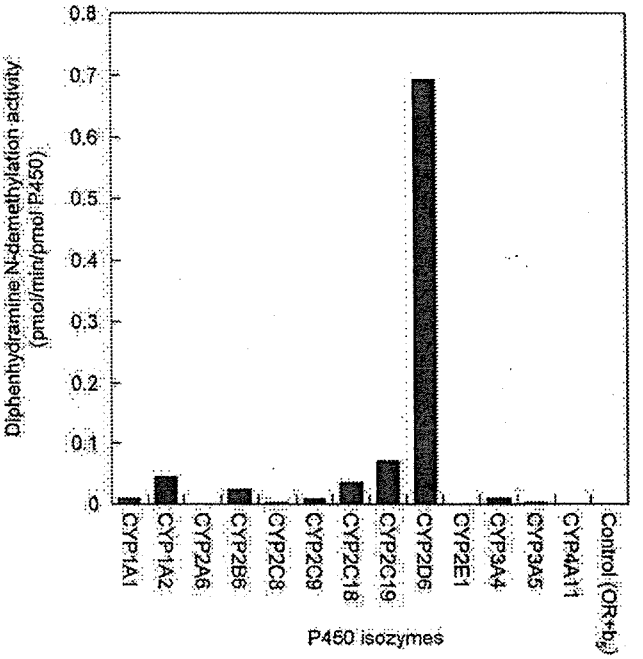

FIG. 2. Diphenhydramine *N*-demethylation activity at 0.5 μM in microsomes of baculovirus-infected insect cells expressing 14 different P450 isozymes individually. Five pmol/ml recombinant P450 isozyme was incubated with 0.5 μM diphenhydramine at 37°C for 20 min. The incubation was performed in the presence of NADPH. Recombinant P450 isozymes used in the present study were coexpressed with cytochrome P450 oxidoreductase and/or cytochrome b_5. The amounts of cytochrome P450 oxidoreductase and cytochrome b_5 of the recombinant P450 isozymes used in the present study were 250 to 4900 nmol/min/mg protein and 200 to 1000 pmol/mg protein, respectively. Each column represents the mean of two independent analyses. *b5*, cytochrome b_5; OR, cytochrome P450 oxidoreductase.

Kinetics of Diphenhydramine *N*-Demethylation Activity in Pooled Human Liver Microsomes. The Eadie-Hofstee plot for diphenhydramine *N*-demethylation activity in pooled human liver microsomes showed a biphasic pattern (data not shown). V_{max1} and K_{m1}, kinetic parameters for the high-affinity component, were calculated to be 30.2 pmol/min/mg protein and 13.3 μM, respectively. V_{max2} and K_{m2}, kinetic parameters for the low-affinity component, were calculated to be 551 pmol/min/mg protein and 401 μM, respectively. Each parameter was calculated by the mean of three independent analyses.

Diphenhydramine *N*-Demethylation Activity in Individual Human Liver Microsomes. As shown in Fig. 3, diphenhydramine *N*-demethylation activities at 0.5 μM varied 4.5-fold (0.87–3.89 pmol/min/mg protein) among 12 human liver microsomes tested. Diphenhydramine *N*-demethylation activity in human liver microsomes was completely inhibited by SKF-525A (1 mM), a typical P450 inhibitor, which was incubated concomitantly with diphenhydramine and was not detected in the absence of the NADPH generating system (data not shown).

Correlations between Diphenhydramine *N*-Demethylation Activity in the Presence or Absence of Quinidine and Specific Activities of Other P450 Isozymes in Human Liver Microsomes. As shown in Table 1, correlation coefficients between diphenhydramine *N*-demethylation activities in the presence or absence of 1 μM quinidine and specific activities of other P450 isozymes were calculated in human liver microsomes from 12 individual donors. In the absence of quinidine, diphenhydramine *N*-demethylation activity was signifi-

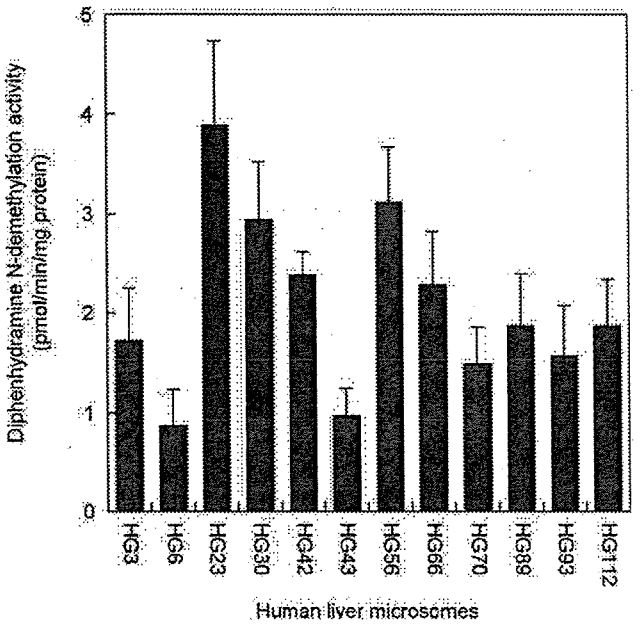

FIG. 3. Diphenhydramine *N*-demethylation activity at 0.5 μM in human liver microsomes from 12 individual donors. Human liver microsomal protein (0.1 mg/ml) was incubated with 0.5 μM diphenhydramine at 37°C for 60 min. The incubation was performed in the presence of NADPH. The amounts of cytochrome P450 oxidoreductase and cytochrome b_5 of the human liver microsomes used in the present study were 241 to 415 nmol/min/mg protein and 445 to 754 pmol/mg protein, respectively. Each column represents the mean ± S.D. of five independent analyses.

TABLE 1

Correlations of diphenhydramine N-demethylation activity in the presence or absence of quinidine with P450 isozyme-specific activities in human liver microsomes from 12 individual donors

The correlation coefficients (r) were calculated by the least-squares regression method.

P450 Isozyme	Specific Activity	r	
		Without Quinidine	With Quinidine
CYP1A2	Phenacetin *O*-deethylation	0.468	0.721**
CYP2A6	Coumarin 7-hydroxylation	0.127	0.177
CYP2B6	(*S*)-Mephenytoin *N*-demethylation	0.099	0.345
CYP2C8	Paclitaxel 6α-hydroxylation	0.143	0.468
CYP2C9	Diclofenac 4′-hydroxylation	0.346	0.822**
CYP2C19	(*S*)-Mephenytoin 4′-hydroxylation	0.027	0.542
CYP2D6	Bufuralol 1′-hydroxylation	0.672*	—
CYP2E1	Chlorzoxazone 6-hydroxylation	0.310	0.050
CYP3A4	Testosterone 6β-hydroxylation	0.072	0.546
CYP4A	Lauric acid 12-hydroxylation	0.616*	0.404

* $p < 0.05$, ** $p < 0.01$ (statistical significance for r).
—, not calculated.

cantly correlated with bufuralol 1′-hydroxylation activity ($r = 0.672$, $p < 0.05$) and lauric acid 12-hydroxylation activity ($r = 0.616$, $p < 0.05$). On the other hand, when CYP2D6 activities were inhibited by quinidine, phenacetin *O*-deethylation activity ($r = 0.721$, $p < 0.01$) and diclofenac 4′-hydroxylation activity ($r = 0.822$, $p < 0.01$) were significantly correlated with residual diphenhydramine *N*-demethylation activity. Percentages of inhibition of diphenhydramine *N*-demethylation by quinidine in human liver microsomes from 12 individual donors were 4.8 to 76.1%.

Inhibition Studies with Furafylline, Sulfaphenazole, and Omeprazole in Individual and Pooled Human Liver Microsomes. Diphenhydramine *N*-demethylation activities in the presence of furafylline, sulfaphenazole, or omeprazole (each 10 μM) were determined in four individual samples and one pooled sample of human liver microsomes. The inhibitory effects of these inhibitors and quinidine on diphenhydramine *N*-demethylation activity are shown in Fig. 4. As shown in Fig. 4B, diphenhydramine *N*-demethylation of HG66, having a high bufuralol 1′-hydroxylation activity, was hardly inhibited by furafylline (5.9%), sulfaphenazole (5.8%), or omeprazole (6.2%). In HG30, having no detectable bufuralol 1′-hydroxylation activity and high phenacetin *O*-deethylation and diclofenac 4′-hydroxylation activity, diphenhydramine *N*-demethylation was inhibited by furafylline (53.1%), sulfaphenazole (39.2%), and omeprazole (46.7%) (Fig. 4A). In HG89, having a low bufuralol 1′-hydroxylation activity and medium phenacetin *O*-deethylation, diclofenac 4′-hydroxylation and (*S*)-mephenytoin 4′-hydroxylation activity, diphenhydramine *N*-demethylation was inhibited by furafylline (56.0%), sulfaphenazole (25.8%), and omeprazole (37.0%) (Fig. 4C). In HG112, having low bufuralol 1′-hydroxylation and phenacetin *O*-deethylation activity and high diclofenac 4′-hydroxylation and (*S*)-mephenytoin 4′-hydroxylation activity, diphenhydramine *N*-demethylation was inhibited by furafyl-

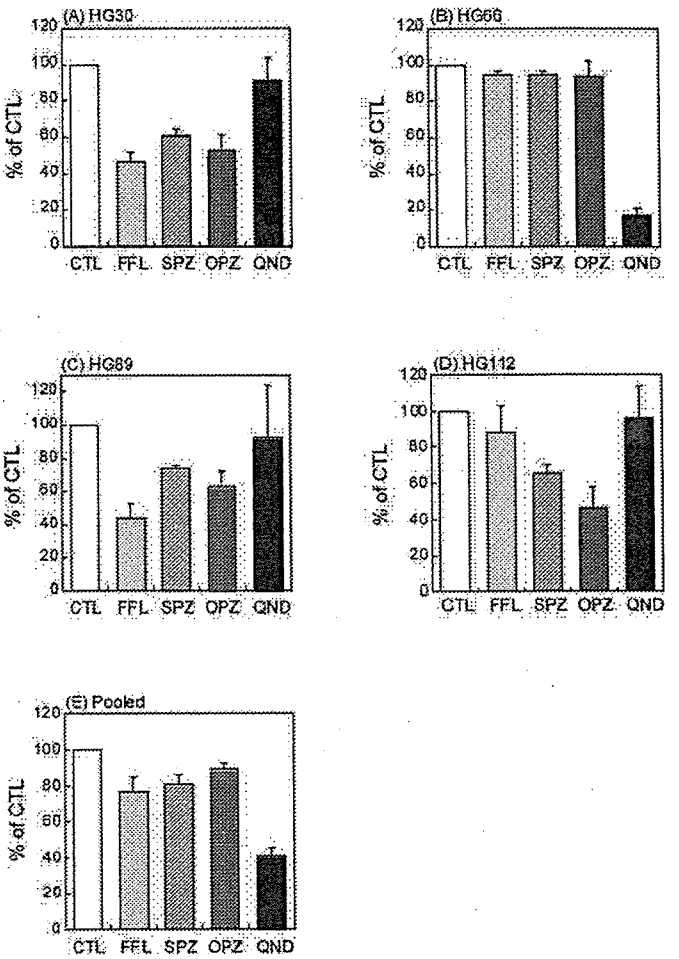

FIG. 4. Effects of furafylline, sulfaphenazole, omeprazole, and quinidine on diphenhydramine *N*-demethylation in individual and pooled human liver microsomes. Individual human liver microsomes (HG33, 66, 89, and 112) and pooled human liver microsomes were incubated with 0.5 μM diphenhydramine and P450 isozyme-specific inhibitors (10 μM furafylline, sulfaphenazole, or omeprazole or 1 μM quinidine) at 37°C for 60 min. Each value is the percentage of residual activity compared with the control sample (containing no inhibitor). The control activities of diphenhydramine *N*-demethylation of individual (HG30, 66, 89, and 112) and pooled human liver microsomes were 3.34 ± 0.44, 2.24 ± 0.19, 1.87 ± 0.15, 2.17 ± 0.39, and 1.41 ± 0.13 pmol/min/mg protein, respectively. Each column expresses the mean ± S.D. of three or four independent analyses. CTL, control; FFL, furafylline; SPZ, sulfaphenazole; OPZ, omeprazole; QND, quinidine.

TABLE 2

Michaelis-Menten kinetic parameters of diphenhydramine N-demethylation in baculovirus-infected insect cells expressing CYP1A2, CYP2C9, CYP2C19, or CYP2D6

Data represent mean ± S.D. of three independent analyses.

P450 Isozyme	V_{max}	K_m	V_{max}/K_m
	pmol/min/pmol P450	*μM*	*μl/min/pmol P450*
CYP1A2	14.0 ± 2.3	295 ± 46	0.047
CYP2C9	4.43 ± 0.28	134 ± 32	0.033
CYP2C19	11.0 ± 2.6	55.7 ± 6.5	0.198
CYP2D6	2.38 ± 0.24	1.12 ± 0.21	2.13

line (11.8%), sulfaphenazole (34.8%), and omeprazole (54.1%) (Fig. 4D). In pooled human liver microsomes, diphenhydramine *N*-demethylation was inhibited by furafylline (23.0%), sulfaphenazole (19.7%), and omeprazole (11.2%) (Fig. 4E).

Kinetics of Diphenhydramine *N*-Demethylation in Recombinant CYP1A2, CYP2C9, CYP2C19, and CYP2D6. Concentration-activity relationships for diphenhydramine *N*-demethylation activities of recombinant CYP1A2, CYP2C9, CYP2C19, and CYP2D6 were able to be fitted by a Michaelis-Menten equation. The kinetic parameters in recombinant CYP1A2, CYP2C9, CYP2C19, and CYP2D6 are listed in Table 2. The V_{max} value of recombinant CYP2D6 was 2.38 ± 0.24 pmol/min/pmol P450. Recombinant CYP2D6 showed the lowest K_m value (1.12 ± 0.21 μM). V_{max} values of CYP1A2, CYP2C9, and CYP2C19 were 14.0 ± 2.3, 4.43 ± 0.28, and 11.0 ± 2.6 pmol/min/pmol P450, respectively. K_m values of CYP1A2, CYP2C9, and CYP2C19 were 295 ± 46, 134 ± 32, and 55.7 ± 6.5 μM, respectively.

Contributions of CYP1A2, CYP2C9, CYP2C19, and CYP2D6 to Diphenhydramine *N*-Demethylation in Human Liver Microsomes. Contributions of CYP2D6, CYP1A2, CYP2C9, and CYP2C19 to diphenhydramine *N*-demethylation in four individual samples and one pooled sample of human liver microsomes estimated by the application of RAFs are shown in Fig. 5A. In HG66, which showed a high level of bufuralol 1′-hydroxylation activity, the contribution of CYP2D6 to diphenhydramine *N*-demethylation was estimated to be up to 80%, whereas the contributions of CYP1A2, CYP2C9, and CYP2C19 were low. In HG30, HG89, and HG112, which showed no detectable or low levels of bufuralol 1′-hydroxylation activity, the contribution of CYP2D6 to diphenhydramine *N*-demethylation was estimated to be negligible or low (0–12.1%). On the other hand, contributions of CYP1A2, CYP2C9, and CYP2C19 in these microsomes were estimated to be relatively high (around 30%) for each isozyme except for CYP1A2 in HG112 (4.2%), which showed a low phenacetin *O*-deethylation activity. In pooled human liver microsomes, the contribution of CYP2D6 was estimated to be half of the total activity of diphenhydramine *N*-demethylation.

Contributions of CYP1A2, CYP2C9, CYP2C19, and CYP2D6 to diphenhydramine *N*-demethylation, estimated by the application of RAFs and by the results of inhibition studies, were compared in Fig. 5, A and B. Contributions of these P450 isozymes to diphenhydramine *N*-demethylation estimated by the application of RAFs (Fig. 5A) were in good agreement with those estimated by inhibition studies using P450 isozyme-specific inhibitors in four individual samples and one pooled sample of human liver microsomes (Fig. 5B).

Discussion

In the present study, the highest level of activity of diphenhydramine *N*-demethylation was found in recombinant CYP2D6 at a clinically relevant concentration (0.5 μM) by an LC/MS method developed in our laboratory (Fig. 2). A significant correlation was also

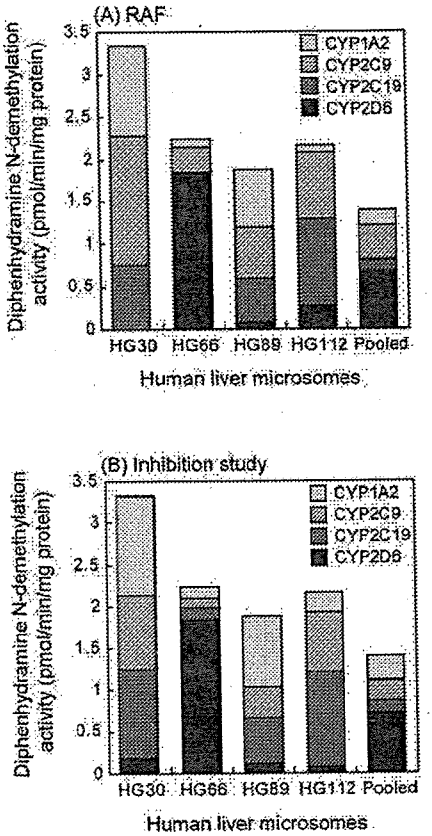

FIG. 5. Comparisons of the contributions of CYP1A2, CYP2C9, CYP2C19, and CYP2D6 to diphenhydramine *N*-demethylation estimated by the application of RAFs and by the results of inhibition studies. Contributions of P450 isozymes to diphenhydramine *N*-demethylation estimated by the application of RAFs (A) and by the results of inhibition studies (B) are shown. Data represent predicted contribution of each P450 isozyme to the total activity of each individual and pooled sample of human liver microsomes. Contributions of CYP1A2, CYP2C9, CYP2C19, and CYP2D6 estimated by the application of RAFs in individual and pooled human liver microsomes are as follows: 31.6, 45.9, 22.5, and 0%, respectively, in HG30; 4.1, 13.4, 1.2, and 81.3%, respectively, in HG66; 36.0, 32.1, 27.4, and 4.6%, respectively, in HG89; 4.2, 35.8, 47.9, and 12.1%, respectively, in HG112; and 14.2, 27.5, 9.9, and 48.4%, respectively, in pooled human liver microsomes.

found between diphenhydramine *N*-demethylation activity and bufuralol 1′-hydroxylation activity ($r = 0.672$, $p < 0.05$) in human liver microsomes from 12 individual donors (Table 1). Moreover, diphenhydramine *N*-demethylation was strongly inhibited by quinidine in human liver microsomes having a high level of CYP2D6 activity (HG66, Fig. 4B). Furthermore, the K_m value for diphenhydramine *N*-demethylation of recombinant CYP2D6 is the lowest (1.12 ± 0.21 μM) among P450 isozymes tested (Table 2). These results indicate that *N*-demethylation of diphenhydramine is mainly catalyzed by CYP2D6 as a high-affinity P450 isozyme in vitro. In a previous case report, the half-life of diphenhydramine was 2-fold greater than the usual value in an elderly woman who had a prolonged half-life of imipramine (Glassman et al., 1985), which is mainly metabolized by CYP2D6 (Koyama et al., 1997), suggesting that diphenhydramine is a substrate of CYP2D6 in vivo. In addition, diphenhydramine is known to inhibit the metabolism of several other CYP2D6 substrates in vitro and in vivo (Hamelin et al., 1998, 2000; Lessard et al., 2001; He et al., 2002). These findings, coupled with the results of the present study, suggest that diphenhydramine is not only a potent inhibitor of CYP2D6 but also a high-affinity substrate of CYP2D6 in vitro and in vivo.

Since an Eadie-Hofstee plot in pooled human liver microsomes

showed a biphasic pattern, multiple P450 isozymes are thought to be involved in *N*-demethylation of diphenhydramine in addition to CYP2D6. In the present study, we obtained several results supporting the involvement of CYP1A2, CYP2C9, and CYP2C19 in *N*-demethylation of diphenhydramine as low-affinity components. In previous studies (Hamelin et al., 2001; Sharma and Hamelin, 2003), *N*-demethylation of diphenhydramine was reported to be mediated by multiple P450 isozymes, CYP1A2, CYP2C18, CYP2C19, CYP2D6, and CYP2B6, at 20 μM. This finding is consistent with the results of the present study showing that CYP1A2 and CYP2C19 are involved in diphenhydramine *N*-demethylation as low-affinity components, whereas it is inconsistent with the finding in the present study that CYP2C9 is involved as one of the low-affinity enzymes in diphenhydramine *N*-demethylation. However, the results of the present study showed that diclofenac 4′-hydroxylation was significantly correlated with diphenhydramine *N*-demethylation activity ($r = 0.822, p < 0.01$) in human liver microsomes from 12 individual donors when CYP2D6 activity was inhibited by quinidine (Table 1). Furthermore, an inhibitory effect of sulfaphenazole on *N*-demethylation of diphenhydramine was seen in human liver microsomes having low levels of or no detectable activity of CYP2D6 (Fig. 4) and was in good agreement with the contribution of CYP2C9 estimated by application of the RAF (Fig. 5). Therefore, diphenhydramine *N*-demethylation seems to be mediated by CYP2C9 in addition to CYP1A2 and CYP2C19 as low-affinity components in human liver microsomes. In the present study, although a significant correlation was also found between lauric acid 12-hydroxylation and diphenhydramine *N*-demethylation activity (Table 1), involvement of CYP4A was not examined because a correlation was not found when CYP2D6 was inhibited by quinidine (Table 1) and diphenhydramine *N*-demethylation activity was not detectable in recombinant CYP4A11 (Fig. 2). In addition, involvement of CYP2C18 and CYP2B6 was not examined in the present study because the results of inhibition studies using P450 isozyme-specific inhibitors in individual and pooled human liver microsomes showed that low-affinity components involved in *N*-demethylation of diphenhydramine are almost completely explained by CYP1A2, CYP2C9, and CYP2C19 (Fig. 4).

The main adverse effects of classic antihistamines are effects on the central nervous system such as sedation, and impairment of cognitive function and psychomotor performance (Hindmarch and Shamsi, 1999; Welch and Meltzer, 2002). The sedative effect of diphenhydramine has been reported to be correlated with its plasma concentration (Carruthers et al., 1978). Therefore, when the major metabolic process of diphenhydramine and a concomitant drug(s) is mediated by the same P450 isozyme(s), a sedative effect may be induced by an increase in the plasma concentration of diphenhydramine. The results of the present study indicate that diphenhydramine is mainly metabolized by CYP2D6, which is known to catalyze the oxidative metabolism of various clinically important drugs (Zanger et al., 2004). In addition, since diphenhydramine is available without prescription (Food and Drug Administration, 2002), it is possible that it is taken with various drugs. Therefore, it should be emphasized that the plasma concentration of diphenhydramine may be increased and a sedative effect may be induced by coadministration of CYP2D6 substrates/inhibitors. Besides, in the case of poor metabolizer phenotypes of CYP2D6, drug-drug interaction may occur between diphenhydramine and substrates/inhibitors/inducers of CYP1A2, CYP2C9, and CYP2C19, because *N*-demethylation of diphenhydramine seems to be mediated by these P450 isozymes as low-affinity components.

In the present study, diphenhydramine *N*-demethylation activities at 0.5 μM varied 4.5-fold (0.87–3.89 pmol/min/mg protein) among human liver microsomes tested (Fig. 5). In addition, the results of the present study indicate that diphenhydramine *N*-demethylation is mainly catalyzed by CYP2D6. Therefore, the plasma concentration of diphenhydramine is thought to be influenced by the metabolic activity of CYP2D6, which varies extensively among individuals who can be categorized on the basis of their CYP2D6 activity as ultrarapid, extensive, intermediate, and poor metabolizers, which are reflected by *CYP2D6* genetic polymorphism (Zanger et al., 2004). However, a previous study showed that the clearance of diphenhydramine to its *N*-demethylated metabolite was not different in extensive and poor metabolizer phenotypes of CYP2D6 (Lessard et al., 2001). Although the reason for this discrepancy is unclear, in the case of poor metabolizer phenotypes of CYP2D6, individual differences in plasma concentration of diphenhydramine could be caused by large differences in metabolic activities of CYP1A2, CYP2C9, and CYP2C19 (Chiba, 1998; Furuta et al., 2005; Kirchheiner and Brockmoller, 2005). Furthermore, CYP1A2 is known to be a P450 isozyme inducible by environmental factors such as polycyclic aromatic hydrocarbons (Sherson et al., 1992; Pelkonen et al., 1998). Therefore, the effects of genetic polymorphisms of CYP2D6 on the disposition of diphenhydramine may be masked by the interindividual differences in the metabolic capacity of these P450 isozymes. Further studies are needed to clarify the involvement of CYP2D6 in the metabolism of diphenhydramine *N*-demethylation as a major enzyme in vivo. Such study is now under way in our laboratory.

In conclusion, *N*-demethylation of diphenhydramine is mainly catalyzed by CYP2D6 as a high-affinity P450 isozyme at a clinically relevant concentration. Therefore, it seems that diphenhydramine is not only a potent inhibitor of CYP2D6 but also a high-affinity substrate of CYP2D6. It should be noted that the sedative effect of diphenhydramine might be caused by an increase in the plasma concentration of diphenhydramine by concomitant use of CYP2D6 substrates/inhibitors. In addition, CYP1A2, CYP2C9, and CYP2C19 are involved in the metabolism of diphenhydramine as low-affinity P450 isozymes. Therefore, it should also be noted that diphenhydramine might interact with substrates/inhibitors/inducers of these P450 isozymes in the case of poor or intermediate metabolizer phenotype of CYP2D6.

References

Blyden GT, Greenblatt DJ, Scavone JM, and Shader RI (1986) Pharmacokinetics of diphenhydramine and demethylated metabolite following intravenous and oral administration. *J Clin Pharmacol* **26**:529–533.

Bourrie M, Meunier V, Berger Y, and Fabre G (1996) Cytochrome P450 isoform inhibitors as a tool for the investigation of metabolic reactions catalyzed by human liver microsomes. *J Pharmacol Exp Ther* **277**:321–332.

Carruthers SG, Shoeman DW, Hignite CE, and Azarnoff DL (1978) Correlation between plasma diphenhydramine level and sedative and antihistamine effects. *Clin Pharmacol Ther* **23**:375–382.

Chang T, Okerholm RA, and Glazko AJ (1974) Identification of diphenhydramine (Benadryl) metabolites in human subjects. *Res Commun Chem Pathol Pharmacol* **9**:391–404.

Chiba K (1998) Genetic polymorphism of the CYP2C subfamily. *Nippon Yakurigaku Zasshi* **112**:15–21.

Crespi CL (1995) Xenobiotic-metabolizing human cells as tools for pharmacological and toxicological research. *Adv Drug Res* **26**:179–235.

de Groot MJ, Bijloo GJ, Martens BJ, van Acker FAA, and Vermeulen NPE (1997) A refined substrate model for human cytochrome P450 2D6. *Chem Res Toxicol* **10**:41–48.

Food and Drug Administration (2002) Labeling of diphenhydramine-containing drug products for over-the-counter human use. Final rule. *Fed Regist* **67**:72555–72559.

Furuta T, Shirai N, Sugimoto M, Nakamura A, Hishida A, and Ishizaki T (2005) Influence of CYP2C19 pharmacogenetic polymorphism on proton pump inhibitor-based therapeutics. *Drug Metab Pharmacokinet* **20**:153–167.

Giraud C, Tran A, Rey E, Vincent J, Treluyer JM, and Pons G (2004) In vitro characterization of clobazam metabolism by recombinant cytochrome P450 enzymes: importance of CYP2C19. *Drug Metab Dispos* **32**:1279–1286.

Glassman JN, Dugas JE, Tsuang MT, and Loyd DW (1985) Idiosyncratic pharmacokinetics complicating treatment of major depression in an elderly woman. *J Nerv Ment Dis* **173**:573–576.

Hamelin BA, Bouayad A, Drolet B, Gravel A, and Turgeon J (1998) In vitro characterization of cytochrome P450 2D6 inhibition by classic histamine H_1 receptor antagonists. *Drug Metab Dispos* **26**:536–539.

Hamelin BA, Bouayad A, Methot J, Jobin J, Desgagnes P, Poirier P, Allaire J, Dumesnil J, and Turgeon J (2000) Significant interaction between the nonprescription antihistamine diphen-

hydramine and the CYP2D6 substrate metoprolol in healthy men with high or low CYP2D6 activity. *Clin Pharmacol Ther* **67**:466–477.
Hamelin BA, Rioux N, Gauvin C, Pilote S, and Winocour PD (2001) Multiple cytochrome P450 enzymes and FMO1 are implicated in the metabolism of diphenhydramine. *Drug Metab Rev* **33 (Suppl 1)**:91.
He N, Zhang WQ, Shockley D, and Edeki T (2002) Inhibitory effects of H_1-antihistamines on CYP2D6- and CYP2C9-mediated drug metabolic reactions in human liver microsomes. *Eur J Clin Pharmacol* **57**:847–851.
Hindmarch I and Shamsi Z (1999) Antihistamines: models to assess sedative properties, assessment of sedation, safety and other side-effects. *Clin Exp Allergy* **29 (Suppl 3)**:133–142.
Kay GG and Quig ME (2001) Impact of sedating antihistamines on safety and productivity. *Allergy Asthma Proc* **22**:281–283.
Kirchheiner J and Brockmoller J (2005) Clinical consequences of cytochrome P450 2C9 polymorphisms. *Clin Pharmacol Ther* **77**:1–16.
Kobayashi K, Nakajima M, Oshima K, Shimada N, Yokoi T, and Chiba K (1999) Involvement of CYP2E1 as a low-affinity enzyme in phenacetin O-deethylation in human liver microsomes. *Drug Metab Dispos* **27**:860–865.
Koyama E, Chiba K, Tani M, and Ishizaki T (1997) Reappraisal of human CYP isoforms involved in imipramine N-demethylation and 2-hydroxylation: a study using microsomes obtained from putative extensive and poor metabolizers of S-mephenytoin and eleven recombinant human CYPs. *J Pharmacol Exp Ther* **281**:1199–1210.
Koymans L, Vermeulen NP, van Acker SA, te Koppele JM, Heykants JJ, Lavrijsen K, Meuldermans W, and Donne-Op den Kelder GM (1992) A predictive model for substrates of cytochrome P450-debrisoquine (2D6). *Chem Res Toxicol* **5**:211–219.
Lessard E, Yessine MA, Hamelin BA, Gauvin C, Labbe L, O'Hara G, LeBlanc J, and Turgeon J (2001) Diphenhydramine alters the disposition of venlafaxine through inhibition of CYP2D6 activity in humans. *J Clin Psychopharmacol* **21**:175–184.
Loew ER, MacMillan R, and Kaiser ME (1946) The anti-histamine properties of Benadryl, beta-dimethylaminoethyl benzhydryl ether hydrochloride. *J Pharmacol Exp Ther* **86**:229–238.
Miyaguchi H, Kuwayama K, Tsujikawa K, Kanamori T, Iwata YT, Inoue H, and Kishi T (2006) A method for screening for various sedative-hypnotics in serum by liquid chromatography/single quadrupole mass spectrometry. *Forensic Sci Int* **157**:57–70.
Mizushima Y (2006) Antihistamines, in *Today's Drug Therapy*, pp 301–323, Nankodo, Tokyo, Japan.
Monahan BP, Ferguson CL, Killeavy ES, Lloyd BK, Troy J, and Cantilena LR Jr (1990) Torsades de pointes occurring in association with terfenadine use. *J Am Med Assoc* **264**:2788–2790.
Nakamura K, Yokoi T, Inoue K, Shimada N, Ohashi N, Kume T, and Kamataki T (1996) CYP2D6 is the principal cytochrome P450 responsible for metabolism of the histamine H1 antagonist promethazine in human liver microsomes. *Pharmacogenetics* **6**:449–457.
Nakamura K, Yokoi T, Komada T, Inoue K, Nagashima K, Shimada N, Shimizu T, and Kamataki T (1998) Oxidation of histamine H1 antagonist mequitazine is catalyzed by cytochrome P450 2D6 in human liver microsomes. *J Pharmacol Exp Ther* **284**:437–442.
Paakkari I (2002) Cardiotoxicity of new antihistamines and cisapride. *Toxicol Lett* **127**:279–284.
Pelkonen O, Maenpaa J, Taavitsainen P, Rautio A, and Raunio H (1998) Inhibition and induction of human cytochrome P450 (CYP) enzymes. *Xenobiotica* **28**:1203–1253.
Sharma A and Hamelin BA (2003) Classic histamine H_1 receptor antagonists: a critical review of their metabolic and pharmacokinetic fate from bird's eye view. *Curr Drug Metab* **4**:105–129.
Sherson D, Sigsgaard T, Overgaard E, Loft S, Poulsen HE, and Jongeneelen FJ (1992) Interaction of smoking, uptake of polycyclic aromatic hydrocarbons, and cytochrome P450IA2 activity among foundry workers. *Br J Ind Med* **49**:197–202.
Smith DA and Jones BC (1992) Speculations of the substrate structure-activity relationship (SSAR) of cytochrome P450 enzymes. *Biochem Pharmacol* **44**:2089–2098.
Welch MJ and Meltzer EO (2002) H_1-antihistamines and the central nervous system. *Clin Allergy Immunol* **17**:337–388.
Yasuda SU, Zannikos P, Young AE, Freid KM, Wainer IW, and Woosley RL (2001) The roles of CYP2D6 and stereoselectivity in the clinical pharmacokinetics of chlorpheniramine. *Br J Clin Pharmacol* **53**:519–525.
Zanger UM, Raimundo S, and Eichelbaum M (2004) Cytochrome P450 2D6: overview and update on pharmacology, genetics, biochemistry. *Naunyn-Schmiedeberg's Arch Pharmacol* **369**:23–37.

Address correspondence to: Tomoko Akutsu, Laboratory of Pharmacology and Toxicology, Graduate School of Pharmaceutical Sciences, Chiba University, 1-8-1, Inohana, Chuo-ku, Chiba-shi, Chiba 260-8675, Japan. E-mail: tomoko@nrips.go.jp

J Hum Genet (2007) 52:117–122
DOI 10.1007/s10038-006-0087-0

Human organic cation transporter (*OCT1* and *OCT2*) gene polymorphisms and therapeutic effects of metformin

Eriko Shikata · Rei Yamamoto · Hiroshi Takane · Chiaki Shigemasa · Tadasu Ikeda · Kenji Otsubo · Ichiro Ieiri

Received: 25 August 2006 / Accepted: 27 October 2006 / Published online: 17 November 2006

Abstract Organic cation transporters (OCTs) are responsible for the hepatic and renal transport of metformin. In this study we analyzed variants of *OCT1* and *OCT2* genes in 33 patients (24 responders and nine non-responders) based on the hypothesis that polymorphisms in both genes contribute to large inter-patient variability in the clinical efficacy of metformin. The sequences of the 5′-flanking and coding regions of the two genes of interest were screened by single-strand conformation polymorphism (SSCP) analysis. To compare the causative factors between responders and non-responders, we performed stepwise discriminant functional analysis. Age, body mass index (BMI) and treatment with lipid-lowering agents were demonstrated as positive predictors, and two mutations in the *OCT1* gene, –43T > G in intron 1 and 408Met > Val (1222A > G) in exon 7, were negative and positive predictors, respectively, for the efficacy of metformin; the predictive accuracy was 55.5% ($P < 0.05$). Subsequent study indicated that OCT1 mRNA levels tended to be lower in human livers with the 408Met (1222A) variant, though the differences did not reach the level of significance. In this study it is suggested that *OCT1* and *OCT2* gene polymorphisms have little contribution to the clinical efficacy of metformin.

Keywords Metformin · OCT1 · OCT2 · Polymorphisms · Pharmacokinetics · Pharmacodynamics

E. Shikata · H. Takane · K. Otsubo · I. Ieiri
Department of Hospital Pharmacy, Faculty of Medicine, Tottori University, Yonago, Japan

R. Yamamoto · C. Shigemasa
Department of Molecular Medicine and Therapeutics, Faculty of Medicine, Tottori University, Yonago, Japan

T. Ikeda
Department of Adult and Elderly Nursing, Faculty of Medicine, Tottori University, Yonago, Japan

Present Address:
I. Ieiri (✉)
Department of Clinical Pharmacokinetics, Graduate School of Pharmaceutical Sciences, Kyushu University, 3-1-1, Maidashi, Higashi-ku, Fukuoka 812-8582, Japan
e-mail: ieiri-ttr@umin.ac.jp

Introduction

Metformin is one of the most commonly used drugs for the treatment of type 2 diabetes, but we sometimes encounter patients who do not respond sufficiently, even under approved dosage conditions (e.g., 500–750 mg/day in Japan). Although the effects of metformin on glycemic control and lipids have been reported to be dose dependent, recent pharmacogenomic studies indicate that genetic polymorphisms of drug-metabolizing enzymes and transporters should be taken into consideration when large inter-patient variability in the intensity and duration of both drug effects and side effects is observed. Among various pharmacokinetic-related genes, since renal secretion, not hepatic metabolism, is the major route of elimination of metformin, the contribution of genetic variations in drug transporters is of interest.

Human organic cation transporters (OCTs; OCT1–3) are poly-specific transporters of small and hydrophilic

organic cations, including toxic substances, endogenous compounds (e.g., dopamine and serotonin), and clinically used drugs (e.g., procainamide and amantadine) (Jonker and Schinkel 2004). Among the OCT family, OCT1 is expressed predominantly in the basolateral membrane of hepatocytes, and mouse Oct1, which is homologically and functionally similar to OCT1, is responsible for the hepatic uptake of metformin (Wang et al. 2002, 2003). Although the precise mechanism of the action of metformin remains unclear, it is believed that hepatic uptake is an essential step in reducing hepatic glucose production as well as the occurrence of life-threatening side effects such as lactic acidosis (Hundal et al. 2000; Stumvoll et al. 1995; Wang et al. 2002). Recently, a number of single nucleotide polymorphisms (SNPs) has been identified in the *OCT1* gene. Some of these SNPs have been found to be associated with altered in vitro transport activity (Hundal et al. 2000; Sakata et al. 2003; Shu et al. 2003; Takeuchi et al. 2003).

In the kidney, OCT2, another subfamily of the OCT family, is expressed on the basolateral membrane of the proximal tubule epithelium and is involved in the uptake of many xenobiotics from the bloodstream into renal epithelial cells (Jonker and Schinkel 2004). Kimura et al. (2005) demonstrated that metformin is a good substrate for OCT2, using HEK293 cells expressing OCT2. Similar to those in the *OCT1* gene, functionally different variants have been identified in the *OCT2* gene (Leabman et al. 2002).

We hypothesized that large inter-patient variability in the clinical efficacy of metformin may occur as a result of variations in *OCT1* and/or *OCT2*. In this report we evaluated the functional significance of genetic polymorphisms of *OCT1* and *OCT2* genes with regard to the efficacy of metformin in patients with type 2 diabetes. To date, no study has addressed the genotype–phenotype relationship in light of *OCT* in humans.

Materials and methods

Study subjects

Thirty-three patients (nine men and 24 women; mean age 60 years, range 29–73 years) treated with metformin for at least 1 month were enrolled. We excluded patients who discontinued metformin because of adverse effects (e.g., diarrhea and headache). There are no generally accepted criteria in the clinical cut-off point to divide patients into responders and non-responders. Thus, we selected the criteria empirically, based on our clinical experiences and a previous report (Takei et al. 2001) as follows: (1) responders [n = 24; mean age 62 years, range 29–73 years; mean body mass index (BMI) 25.4 kg/m^2, range 20.4–34.5 kg/m^2], i.e., those whose HbA_{1c} levels had decreased by more than 0.5% from the baseline within 3 months of metformin therapy and had remained low for more than 3 months; and (2) non-responders (n = 9; mean age 56 years, range 34–69 years; mean BMI 25.1 kg/m^2, range 17.8–30.6 kg/m^2), i.e., those for whom either metformin therapy had been discontinued within 3 months and/or after another hypoglycemic drug (e.g., sulfonylurea) had been added to the therapy because of insufficient improvement in HbA_{1c} levels. Eighteen of the responders and six of the non-responders were treated with the maximum approved daily dose in Japan (i.e., 750 mg/day). Eight of the responders and four of the non-responders received metformin monotherapy, and others were co-medicated with sulfonylurea, α-glycosidase inhibitor or insulin. This study was approved by the Ethics Review Board of the Faculty of Medicine, Tottori University, and all subjects gave informed consent before participating.

Identification of variants in *OCT1* and *OCT2* genes

Genomic DNA was extracted from peripheral blood. The primer design was based on the sequence of the 5'-flanking region and the intron/exon junction of *OCT1* and *OCT2* genes (GenBank accession number AL353625 for *OCT1*, AL162582 for *OCT2*). Primers were designed to divide all 11 exons of each gene into fragments of approximately 350 bp so that mutations could be screened by subsequent single-strand conformation polymorphism (SSCP) analysis. Polymerase chain reaction (PCR) products were sequenced either directly or after subcloning on an ABI 3100 automatic sequencer (Applied Biosystems, Foster City, VA, USA).

Quantitative real-time PCR

Total RNA was extracted with an RNAeasy kit (Qiagen, Hilden, Germany) from 58 human liver samples (33 Caucasian and 25 Japanese non-diabetic donors), and reverse transcribed into cDNA using oligo dT primers and reverse transcriptase. OCT1 mRNA was quantified by real-time PCR using an ABI PRISM 7700 sequence detector (Applied Biosystems) with SYBR-green detection of reaction products. Primers for OCT1 mRNA were directed at a sequence that spans the junction of exons 9 and 10, corresponding to open reading frame 1437–1509; 5'-CAC

CCCCTTCATAGTCTTCAG-3′ (forward) and 5′-GCC CAACACCGCAAACAAAAT-3′ (reverse). The copy number of the transcript was measured against the copy-number standard curve of cloned target templates consisting of serial tenfold dilution points. β_2-microglobin mRNA was used as the reference gene for OCT1 mRNA.

Statistical analysis

The significance of differences in allelic frequency was calculated by χ^2 analysis using 2 × 2 contingency tables. Statistical differences among the data for each group were determined by analysis of variance (ANOVA), followed by the Fisher least significant difference test. To compare the causative factors between responders and non-responders, we performed stepwise discriminant functional analysis. At each step, improvement in the χ^2 and the P values was used to check whether the variable entered at that step significantly improved the discrimination. The independent variables were as follows: polymorphisms, gender, age, duration of disease, types and numbers of co-medicated anti-hyperglycemic drugs, daily dose of metformin, BMI, aspartate aminotransferase, alanine aminotransferase, total cholesterol, high-density lipoprotein (HDL) and treatment with lipid-lowering agents (statins and fibrates). Data are shown as means ± SDs. A P value <0.05 was considered to be significant.

Results

Although the time course of change in the mean daily dose of metformin (milligrams per kilogram per day) and the initial level of HbA_{1c} did not differ between the two groups, the mean HbA_{1c} level was significantly lower in the responder group than in the non-responder group during metformin therapy (Fig. 1).

To identify polymorphisms, we performed PCR–SSCP analysis of all 11 exons of the two genes of interest (*OCT1* and *OCT2*), using DNA obtained from all patients, and the allelic frequency was compared between the responder and non-responder groups. In the *OCT1* gene, 11 polymorphisms were detected by SSCP analysis and identified by subsequent sequencing; none were novel polymorphisms (Table 1). Of these, five SNPs resulted in the following amino acid substitutions: 123C > G (41Phe > Leu), 350C > T (117Pro > Leu), 480C > G (160Phe > Leu), 1022C > T (341Pro > Leu), and 1222A > G (408Met > Val). Although 480C > G, 1022C > T, and 1222A > G variants had a relatively

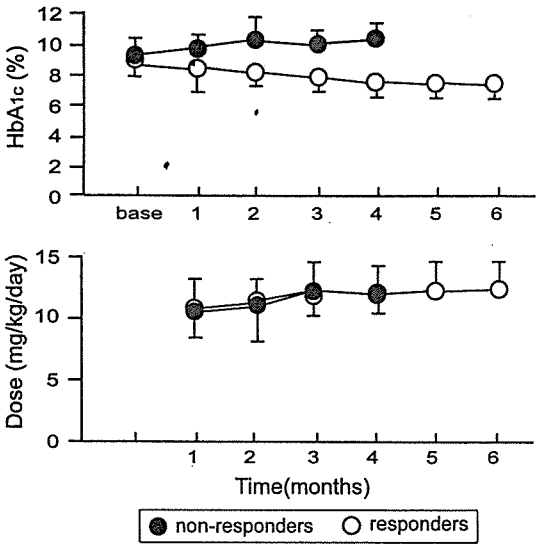

Fig. 1 Time course of changes in HbA_{1c} and metformin daily dose during the observation period in responders and non-responders

high incidence, 123C > G and 350C > T were observed in one patient as heterozygosity. In the *OCT2* gene, two non-synonymous variants were observed: 602C > T (201Thr > Met) and 808G > T (270Ala > Ser). Altogether, there were no remarkable differences in the prevalence of any mutation between responders and non-responders.

The result of discriminant functional analysis is shown in Table 2. Variables selected by the discriminant process were age, BMI, treatment with lipid-lowering agents and two mutations in the *OCT1* gene (–43T > G and 1222A > G). Other variables, such as duration of disease, daily dose of metformin, and types of co-medicated anti-hyperglycemic drugs, had no significant effect on the discrimination. Although age, BMI and treatment with lipid-lowering agents were demonstrated as positive predictors, –43T > G and 1222A > G (408Met > Val) were negative and positive predictors, respectively, for the efficacy of metformin. Total predictive accuracy using these factors was 55.5% ($\chi^2 = 5.59$, $P < 0.05$).

As shown in Table 1, since the frequency of the 408Met allele tended to be higher in non-responders than in responders (0.28 vs 0.19), and since the non-synonymous 408Met > Val variant was selected as a positive predictor, we next examined the association of the 408Met > Val (1222A > G) variant with the expression of OCT1 mRNA in the human liver samples (Fig. 2). Of 58 samples, we analyzed 31 that were homozygotes for the –43T variant (–43T/T). The mean (± SD) hepatic expression level of OCT1 in homozygotes for 408Met (1222A/1222A), heterozygotes for

Table 1 Summary of *OCT1* and *OCT2* gene polymorphisms

Gene	Location	Position[a]	Allele[a]	Nucleotide sequence	Amino acid substitution	Allelic frequency (95% CI)	
						Responders (n = 24)	Non-responders (n = 9)
OCT1	Exon 1	123	C	tcttCctgg	41Phe > Leu	0.98 (0.94–1.02)	1.000
			G	tcttGctgg		0.02 (–0.02–0.06)	0.000
		156	T	agagTcctg	Ser52	0.58 (0.44–0.72)	0.44 (0.21–0.67)
			C	agagCcctg		0.42 (0.28–0.56)	0.56 (0.33–0.79)
		243	C	cgggCgagg	Gly81	1.000	0.94 (0.84–1.05)
			T	cgggTgagg		0.000	0.06 (–0.05–0.16)
		350	C	ctgcCgctg	117Pro > Leu	1.000	0.94 (0.84–1.05)
			T	ctgcTgctg		0.000	0.06 (–0.05–0.16)
	Intron 1	–43	T	atggTtctg	–	0.42 (0.28–0.56)	0.33 (0.12–0.55)
			G	atggGtctg		0.58 (0.44–0.72)	0.67 (0.45–0.89)
	Exon 2	480	C	tcttCtttg	160Phe > Leu	0.88 (0.78–0.97)	0.83 (0.66–1.01)
			G	tcttGtttg		0.13 (0.03–0.22)	0.17 (–0.01–0.34)
	Exon 6	1022	C	acgcCgcgc	341 Pro > Leu	0.81 (0.70–0.92)	0.89 (0.74–1.03)
			T	acgcTgcgc		0.19 (0.08–0.30)	0.11 (–0.03–0.26)
	Exon 7	1222	A	ggccAtgtc	408Met > Val	0.19 (0.08–0.30)	0.28 (0.07–0.49)
			G	ggccGtgtc		0.81 (0.70–0.92)	0.72 (0.52–0.93)
	Inron 7	+8	Deletion	(ggtaagtt)0		0.81 (0.70–0.92)	0.72 (0.52–0.93)
				(ggtaagtt)1		0.19 (0.08–0.30)	0.28 (0.07–0.49)
	Intron 10	+26	C	actcCgagg		0.98 (0.94–1.02)	1.000
			T	actcTgagg		0.02 (–0.02–0.06)	0.000
		–21	C	ccaaCttt		0.46 (0.32–0.60)	0.39 (0.16–0.61)
			T	ccaaTttt		0.54 (0.40–0.68)	0.61 (0.39–0.84)
OCT2	Exon 3	602	C	tataCgtgg	201Thr > Met	0.98 (0.94–1.02)	0.94 (0.84–1.05)
			T	tataTgtgg		0.02 (–0.02–0.06)	0.06 (–0.05–0.16)
	Exon 4	808	G	agttGctct	270Ala > Ser	0.92 (0.88–0.96)	0.94 (0.84–1.05)
			T	agttTctct		0.08 (0.04–0.12)	0.06 (–0.05–0.16)

[a] Position is relative to the ATG start site, and the reference allele for each gene was obtained from the GenBank accession numbers AL353625 for OCT1 and AL162582 for OCT2

408Met > Val (1222A/1222G), and homozygotes for 408Val (1222G/1222G) was 0.69 ± 0.43, 0.92 ± 0.53, and 1.01 ± 0.66, respectively. Although the hepatic expression of OCT1 tended to be lower in livers with the 408Met (1222A) variant, the differences did not reach the level of significance. In the –43T > G variant, the mean OCT1 expression level in –43T/T (n = 18), –43T/G (n = 8), and –43G/G (n = 10) samples (all harbored the 1222G/1222G allele) was 1.01 ± 0.70, 1.04 ± 0.34, and 1.46 ± 0.53, respectively.

Table 2 Stepwise discriminant functional analysis of the efficacy of metformin

Variable	Coefficient	χ^2 value	P
Age	0.09	5.59	0.05
BMI	0.23		
Treatment with lipid-lowering agents	2.25		
–43T > G (intron 1)	–2.35		
408Met > Val (exon 7)	2.51		

Predictive accuracy = 55.5%

Discussion

In this study we first analyzed mutations in *OCT1* and *OCT2* and then examined the association between polymorphisms in these two genes and the efficacy of metformin, because in vitro studies have indicated that OCT1 and OCT2 are responsible, respectively, for the hepatic and renal transport of metformin (Kimura et al. 2005; Wang et al. 2002, 2003). In contrast to studies in vitro and with animals, there are no data from human studies on the contribution of these polymorphisms to the phenotypes of metformin.

In the *OCT1* gene, all non-synonymous variants except 41Phe > Leu and 117Pro > Leu have already been identified in some racial populations, with a frequency of 0.005–0.81 (Kerb et al. 2002; Shu et al. 2003). The 41Phe > Leu and 117Pro > Leu allele frequencies were relatively low (0.004), and they have already been reported in a Japanese population (Itoda et al. 2004). Recent expression studies have indicated that 341Pro > Leu had decreased ability to transport test compounds, while 160Phe > Leu and 408Met > Val were unchanged (Kerb et al. 2002; Sakata et al. 2003;

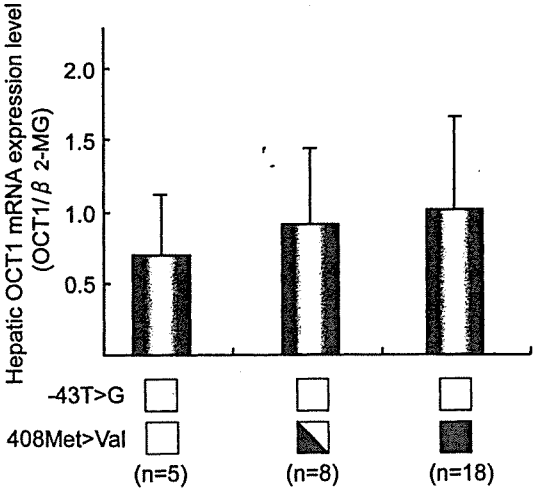

Fig. 2 Hepatic OCT1 mRNA expression levels with regard to the 408Met > Val (1222A > G) variant. Among 58 samples, 31, which were homozygotes for the –43T variant (–43T/T), were analyzed. *Open squares*, *partially filled squares* and *closed squares* correspond to patients homozygous for the 408Met (1222A) allele and heterozygous and homozygous for the 408Val (1222G) allele

Shu et al. 2003). Interestingly, the 341Pro > Leu variant was observed in Asian and African American populations but not in Caucasians (Shu et al. 2003); however, there was no difference in the allele frequency of 341Pro > Leu between responders and non-responders to metformin therapy in this study.

In contrast to those in the *OCT1* gene, it appears that the number of non-synonymous variants in the *OCT2* gene and their allelic frequencies were lower than in other known drug transporter genes such as *MDR1*, *MRP1*, *MRP2*, and *OATP-C* (Nishizato et al. 2003). These observations are consistent with the finding of a lower frequency of non-synonymous variants in ethnically diverse genomic DNA samples (Leabman et al. 2002). Recent population-genetic analysis has demonstrated that selection has acted against amino acid changes in OCT2 (Leabman et al. 2002), suggesting that OCT2 is relatively intolerant of non-synonymous changes. In general, the less frequent non-synonymous variants resulted in more significant and deleterious functional changes. However, the 270Ala > Ser variant was reported to exhibit subtle functional differences from the reference form of OCT2 (Leabman et al. 2002).

Although there were no remarkable differences in the prevalence of any mutation sites between responders and non-responders, we next carried out discriminant functional analysis including not only genetic polymorphisms but also the patients' background. As shown in Table 2, age, BMI and treatment with lipid-lowering agents were demonstrated as positive predictors of metformin efficacy. These observations are partially in agreement with the findings by Knowler et al. (2002), that metformin was less effective in subjects with lower BMI or a lower fasting plasma glucose concentration. BMI > 25 kg/m^2 is defined as obesity in Japan; 66.7% of responders and 44.4% of non-responders were obese in this study. Although the precise mechanism is unknown, these data suggest that metformin is more effective in the case of obesity-induced insulin resistance that is higher fasting plasma glucose. The contribution of lipid-lowering agents was somewhat unexpected, because metformin therapy has been reported to improve both glycemic control and lipid concentrations (i.e., plasma total and low-density lipoprotein cholesterol and triglyceride) in patients with non-insulin-dependent diabetes mellitus (DeFronzo and Goodman 1995). However, in our study, 12 responders and two non-responders were treated with lipid-lowering agents, and most of these patients (11/12 responders and 1/2 non-responders) used HMG-CoA reductase inhibitors (statins). Several studies have shown that low-density lipoprotein (LDL) size rather than plasma LDL level is more correlated with insulin resistance and eventual progression of coronary heart disease (Rizzo and Berneis 2006). Although the efficacy of modifying LDL size is different among agents (fluvastatin and atorvastatin seem to be much more effective agents than pravastatin and simvastatin), statins moderately lower all LDL subclasses, and, somehow, this process seems to make metformin more effective.

Since –43T > G and 408Met > Val (1222A > G) variants were identified as negative and positive predictors, respectively, for the clinical effectiveness of metformin, we evaluated the functional significance of the latter non-synonymous variant in the expression of OCT1 mRNA, using human liver samples. Our findings indicate that samples with the 408Met (1222A) allele tended to be associated with a reduced expression level, as compared with those without the 408Met allele; however, the difference did not reach significance. A recent study using site-directed mutagenesis has indicated that point mutations in the predicted ninth transmembrane domain such as 1222A > G (408Met > Val) do not lead to functional changes (Kerb et al. 2002). We also measured OCT1 mRNA expression with regard to the non-coding –43T > G variant; however, no significant effect was observed. In the present study, the predicted accuracy is still insufficient for its clinical application (i.e., 55.5%). Thus, if these observations are taken into consideration, the contribution of polymorphisms in

OCT1 and *OCT2* genes to metformin efficacy may not be as significant as our expectations had led us to believe. However, since a non-synonymous variant 408Met > Val is often observed simultaneously with other non-synonymous variants (Shu et al. 2003), further in vitro and in vivo studies with regard to the haplotypic consideration, including the non-coding region, are needed to elucidate the functional properties of the variants identified in this study.

While data from only 24 responders and nine non-responders were used, this preliminary investigation is the first study addressing the genotype–phenotype relationship of OCTs in the efficacy of metformin. However, obviously, the small number of patients is a drawback in our study. For example, co-medication of other anti-hyperglycemic drugs in both groups made it difficult for us to judge whether the decreases in HbA_{1c} levels in the responders are attributable to the metformin effect. Clearly, definition of the clinical cut-off point is also essential to divide patients into the two groups correctly. In order to overcome these problems, it is clear that the results in this study should be confirmed in a population study involving large numbers of patients. Nevertheless, this report provides for the possibility of OCTs' functions in humans.

Acknowledgments This work was supported by Health and Labor Sciences Research grants from the Ministry of Health, Labor, and Welfare for Research on Advanced Medical Technology. None of the authors claims any conflict of interest.

References

DeFronzo RA, Goodman AM (1995) Efficacy of metformin in patients with non-insulin-dependent diabetes mellitus. The Multicenter Metformin Study Group. N Engl J Med 333:541–549

Hundal RS, Krssak M, Dufour S, Laurent D, Lebon V, Chandramouli V, Inzucchi SE, Schumann WC, Petersen KF, Landau BR, Shulman GI (2000) Mechanism by which metformin reduces glucose production in type 2 diabetes. Diabetes 49:2063–2069

Itoda M, Saito Y, Maekawa K, Hichiya H, Komamura K, Kamakura S, Kitakaze M, Tomoike H, Ueno K, Ozawa S, Sawada J (2004) Seven novel single nucleotide polymorphisms in the human SLC22A1 gene encoding organic cation transporter 1(OCT1). Drug Metab Pharmacokinet 19:308–312

Jonker JW, Schinkel AH (2004) Pharmacological and physiological functions of the polyspecific organic cation transporters: OCT1, 2, and 3 (SLC22A1–3). J Pharmacol Exp Ther 308:2–9

Kerb R, Brinkmann U, Chatskaia N, Gorbunov D, Gorboulev V, Mornhinweg E, Keil A, Eichelbaum M, Koepsell H (2002) Identification of genetic variations of the human organic cation transporter hOCT1 and their functional consequences. Pharmacogenetics 12:591–595

Kimura N, Okuda M, Inui K (2005) Metformin transport by renal basolateral organic cation transporter hOCT2. Pharm Res 22:255–259

Knowler WC, Barrett-Connor E, Fowler SE, Hamman RF, Lachin JM, Walker EA, Nathan DM (2002) Reduction in the incidence of type 2 diabetes with lifestyle intervention or metformin. N Engl J Med 346:393–403

Leabman MK, Huang CC, Kawamoto M, Johns SJ, Stryke D, Ferrin TE, DeYoung J, Taylor T, Clark AG, Herskowitz I, Giacomini KM (2002) Pharmacogenetics of Membrane Transporters Investigators: polymorphisms in a human kidney xenobiotic transporter, OCT2, exhibit altered function. Pharmacogenetics 12:395–405

Nishizato Y, Ieiri I, Suzuki H, Kimura M, Kawabata K, Hirota T (2003) Polymorphisms of OATP-C (SLC21A6) and OAT3 (SLC22A8) genes: consequences for pravastatin pharmacokinetics. Clin Pharmacol Ther 73:554–565

Rizzo M, Berneis K (2006) The clinical relevance of low-density-lipoproteins size modulation by statins. Cardiovasc Drugs Ther 20:205–217

Sakata T, Anzai N, Shin HJ, Noshiro R, Hirata T, Yokoyama H (2003) Novel single nucleotide polymorphisms of organic cation transporter 1 (SLC22A1) affecting transport functions. Biochem Biophys Res Commun 313:789–793

Shu Y, Leabman MK, Feng B, Mangravite LM, Huang CC, Stryke D, Kawamoto M, Johns SJ, DeYoung J, Carlson E, Ferrin TE, Herskowitz I, Giacomini KM, Pharmacogenetics of Membrane Transporters Investigators (2003) Evolutionary conservation predicts function of variants of the human organic cation transporter, OCT1. Proc Natl Acad Sci U S A 100:5902–5907

Stumvoll M, Nurjhan N, Perriello G, Dailey G, Gerich JE (1995) Metabolic effects of metformin in non-insulin-dependent diabetes mellitus. N Engl J Med 333:550–554

Takei I, Miyamoto K, Funae O, Ohashi N, Meguro S, Tokui M, Saruta T (2001) Secretion of GIP in responders to acarbose in obese type2 (NIDDM) patients. J Diabetes Complications 15:245–249

Takeuchi A, Motohashi H, Okuda M, Inui K (2003) Decreased function of genetic variants, Pro283Leu and Arg287Gly, in human organic cation transporter hOCT1. Drug Metab Pharmacokinet 18:409–412

Wang DS, Jonker JW, Kato Y, Kusuhara H, Schinkel AH, Sugiyama Y (2002) Involvement of organic cation transporter 1 in the hepatic and intestinal distribution of metformin. J Pharmacol Exp Ther 302:510–515

Wang DS, Kusuhara H, Kato Y, Jonker JW, Schinkel AH, Sugiyama Y (2003) Involvement of organic cation transporter 1 in the lactic acidosis caused by metformin. Mol Pharmacol 63:1–5